DEVELOPMENT AND OPTIMIZATION OF A HIGH-TEMPERATURE GEOPOLYMER BASED ADHESIVE FOR METALLIC SUBSTRATES

A Thesis

by

MATTHEW JAMES WESTWICK

Submitted to the Office of Graduate and Professional Studies of
Texas A&M University
in partial fulfillment of the requirements for the degree of

MASTER OF SCIENCE

Chair of Committee,	Miladin Radovic
Committee Members,	Terry Creasy
	Hong Liang
Head of Department,	Andreas Polycarpou

August 2016

Major Subject: Mechanical Engineering

ABSTRACT

Geopolymers (GPs) are defined as a unique class of inorganic polymers synthesized through polycondensation of monomeric Al and Si species into a complex 3D framework. Due to their good mechanical properties, fire resistance, and low thermal conductivity, much research has been conducted on possible use in construction materials and in fire resistant coatings. Despite the abundance of research on geopolymer based coatings on metallic substrates, very little research has been done on the adhesive properties at both room and high temperature of geopolymer gels on metallic substrates.

In this work, substrates adhered with geopolymer based adhesives were analyzed for surface wettability, adhesive layer thickness, lap shear and tensile strength at room and elevated temperatures. In addition, photographic analysis was conducted through use of optical and electron microscopy with Energy-Dispersive X-Ray Spectroscopy (EDS).

Results of testing are conclusive in showing that geopolymer based adhesives are comparable in tensile and shear strengths to alternative commercially available polymer adhesives at room temperature, while maintaining good performance after exposure to elevated temperatures, i.e., up to 800 °C. Exposure to elevated temperatures appears to cracking in the geopolymer matrix without delamination due to thermal expansion mismatch, leading to a reduced strength adhesive without complete debonding or failure. In addition, it was shown that a Si-O-M oxygen bridge develops between the Si in the geopolymer gel and the metal (M) oxide on the surface leading to increased strength.

ACKNOWLEDGEMENTS

I would like to thank my committee chair, Dr. Miladin Radovic, and my committee members, Dr. Terry Creasy and Dr. Hong Liang, for their guidance and support throughout the course of this research. I would also like to thank Dr. Marci Lizcano, who pioneered many of the techniques used in this work and was never too busy to help me.

Thanks also go to my classmates and colleagues in addition to the department faculty and staff for making my time at Texas A&M University a great experience. I also want to extend my gratitude to the members of the Laboratory for Advanced Ceramics and Composites for their assistance and support.

Finally, thanks to my family and friends for their encouragement and to my fiancée for her patience and love.

NOMENCLATURE

Al	Aluminum
CA	Cyocrylanate
EDS	Energy-Dispersive X-Ray Spectroscopy
FTIR	Fourier Transfer Infrared Spectroscopy
GPs	Geopolymer
K	Potassium
KOH	Potassium Hydroxide
MK	Metakaolin
Na	Sodium
NaOH	Sodium Hydroxide
OM	Optical Microscopy
Si	Silicon
SS	Stainless Steel
Ti	Titanium
SEM	Scanning Electron Microscopy
XPS	X-Ray Photoelectron Spectroscopy

TABLE OF CONTENTS

LIST OF FIGURES

Page

LIST OF TABLES

Page

1 INTRODUCTION

1.1 History of Geopolymers

Inorganic aluminosilicate polymers, usually refer to as “Geopolymers”, are a new class of materials that can be used as alternative binding agents to traditional cements. These materials were believed to be first synthesized by Viktor Glukovsky and his team in Ukraine in the mid-1950s [1]. Although they referred to them as “soil silicate concretes”, Joseph Davidovits coined the term “Geopolymer” during his research in the 1970s that is more commonly used today [2].

Various definitions of Geopolymers can be found in the literature. However, the following definition by Bell et. al probably provides the best description of their nature: “Geopolymers are a class of totally inorganic, alumino-silicate based ceramics that are charge balanced by group I oxides. They are rigid gels, which are made under relatively ambient conditions of temperature and pressure into near-net dimension bodies, and which can subsequently be converted to crystalline or glass-ceramic materials [3].”

It is believed that Geopolymers have been used throughout history for different structural applications. In the early 1980s, Davidovits proposed that the ancient Egyptians developed a geopolymeric reaction to synthesize stone blocks for pyramids over 4500 years ago. Several teams of scientists are still currently doing research to support this theory [4]. In addition, Nuclear Magnetic Resonant (NMR) analysis identified geopolymeric compounds (though different from modern synthesized compounds) inside ancient Roman architectural structures primarily used for storing

water, such as aqueducts and cisterns. These cements were believed to have been synthesized using the alkaline rich volcanic soil of the region [5]. Davidovits suggests that in ancient times, geopolymer based cement may have been used as a cementous material long before Portland cement was developed.

Geopolymers possess many traits that make them ideal candidates for 'green' (i.e. renewable resource) building materials. For example, geopolymers can be synthesized from industrial waste with little to no post processing, and produce no atmospheric carbon dioxide (CO_2) upon synthesis. Portland cement, on the other hand, not only requires high temperatures for activation but also releases CO_2 into the atmosphere during production [6]. Advocates for renewable resources as well as environmental advocates have suggested geopolymer based cements would make an excellent green substitute for today's most common Portland cement based concrete [7, 8]. In addition to their green properties, geopolymers also possess several other significant advantages over other traditional cements; several studies have suggested geopolymer cement be used as a fire resistant coating due to its heat and spallation resistance and low thermal conductivity [9, 10]. Other studies have shown that geopolymer materials possess the characteristics needed to safely contain radioactive material [11]. While geopolymers had not been extensively researched before the 21st century, current research shows they may be able to solve many problems in an inexpensive and efficient manner.

1.2 Chemistry and Structure of Geopolymers

Chemically, Geopolymers can be identified as poly-sialates with empirical formula $M_n[-(SiO_2)_z – AlO_2-]n.w.H_2O$ where M is the alkali metal cation, n is the degree of polymerization, z is the Si/Al ratio (usually 1, 2, 3…), and w is the molar water quantity. It is worth noting here, that the activating metal cation M (usually Na^+ or K^+) is believed to stay in the geopolymer framework cavities close to Al and balance the negative charge of the IV-coordinated $[-AlO_2-]^-$, as illustrated in Figure 1 by the yellow atoms [8].

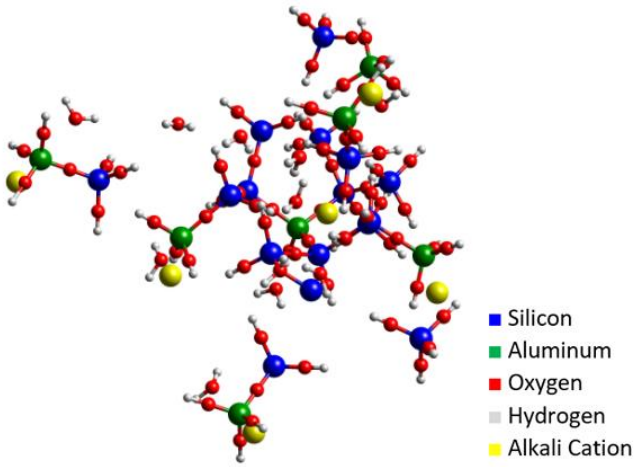

Figure 1: Geopolymer 3D framework [2]

Geopolymers are usually prepared with a Si/Al ratio of 1.8-2.2, an $H_2O/(Al_2O_3 + SiO_2)$ ratio of 2.0-5.0, and a M/Al ratio of 0.9-1.2 (where M is Na or K). Over the last several years, a large number of studies have reported on the effects that chemical composition

of geopolymers has on their structure and properties. Chemical modifications such as water content, additions of other alkali activators, the availability of aluminum, as well as other seemingly insignificant factors can play a large role in the chemical structure, and consequently properties of geopolymers [12-15].

The most studied and arguably the most important factor dictating the properties of geopolymers is the Si/Al ratio in their structure. This ratio dictates the formation of the polysilates that form the geopolymer framework during polycondensation [2, 16, 17]. It is believed that a higher Si:Al ratio allows a more complex interlinking in the geopolymer framework during polycondensation, leading to overall better properties such as higher mechanical strength. Different polysilates for different Si:Al ratios can be seen in Figure 2.

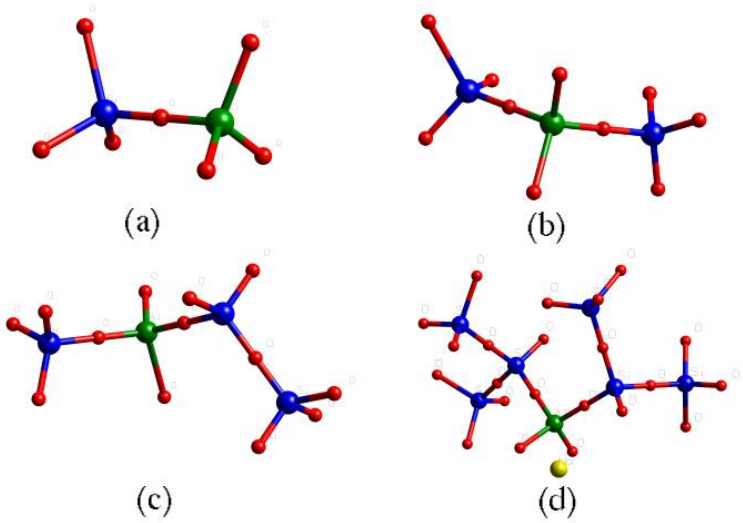

Figure 2: Polysilates corresponding to Si/Al ratios of 1:1, 2:1, 3:1, and 4+:1 [7]

Another critical factor during polycondensation is the availability of aluminum in the geopolymer gel. The amount of aluminum ions is readily available during the polycondensation phase and its release rate directly affect many geopolymer properties, including strength, microstructure, acid resistance, the curing profile, and the strength development profile [18, 19]. While the alumina in metakaolin-based geopolymers is readily available [20], the aluminum ions in fly ash and other industrial waste based geopolymers are much more slowly released. In addition, the release rate can be dictated by alkali activator type and concentration [21]. A slowly released alumina source can become the rate limiting step in a geopolymer reaction, leading to incomplete geopolymerization and polycondensation in addition to slow curing times [22].

High water content affects geopolymers by increasing the distance between the geopolymer chains during polycondensation. Upon curing, this excess water evaporates from the geopolymer leaving a lower density solid with a more open geopolymer framework. By decreasing density, one subsequently decreases compressive strength and increases open porosity. However, open porosity and more open structure can result in lower thermal conductivity [12]. Excessive water also seems to decrease the pH of the alkali solution, thus requiring the addition of extra OH- (usually by adding more NaOH or KOH) to balance the solution and make an optimized geopolymer [8, 23].

The balance of alkali activator to aluminum also seems to be important. Ideally the ratio should be 1:1, as the K+ or Na+ ion is loosely attached to the aluminosilicate framework to balance the positive charge on the Al+ ion. However, an increase in the

alkali/aluminum ratio has been theorized to act as a “chain terminator” during polycondensation and prevent the geopolymer chains from fully developing. In addition, the extra alkaline content makes the geopolymer more hydrophilic and leads to an increase in the residual chemically bonded interstitial water after curing [8, 12, 23].

In another study it was determined that the addition of Calcium, as well as other earth alkaline cations, to the initial geopolymer gel resulted in additional strength at high temperatures. This is partly due to calcium hydroxide creating calcium silicate hydride phases in the aluminosilicate network, developing feldspar and nepheline at high temperatures [24]. Most of the strength increase comes from the tendency toward framework disorder [25]. In addition, calcium and other earth alkali phases act as reaction germs and increase the reaction rate to more quickly develop structure-forming products [24].

Many other chemical considerations in addition to the ones above mentioned have been discussed in the two recent books published on Geopolymers [2, 8].

1.3 Synthesis of Geopolymers

Synthesis of geopolymers is based on Al and Si speciation and condensation polymerization. A basic flowchart of geopolymer synthesis can be seen in Figure 3.

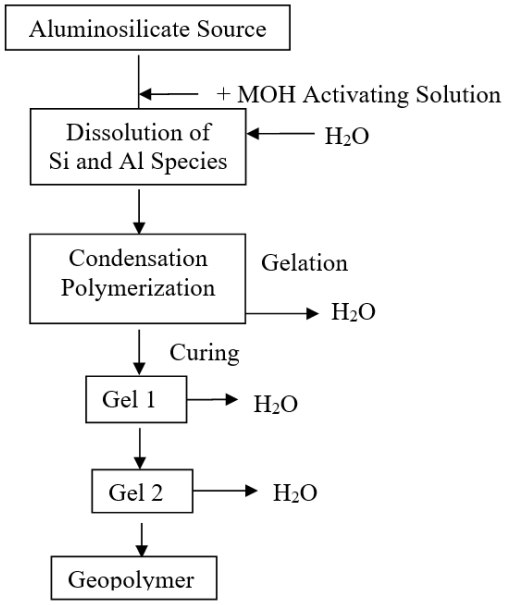

Figure 3: Geopolymerization flowchart [7]

Aluminosilicate rich sources such as clays (i.e. kaolin, or metakaolin) or industrial waste (i.e. fly-ash, steel slag) [26, 27] containing polymeric chemical species, such as $[(SiO)OH_3]^-$, $[(SiO_2)OH_2]^{2-}$, $[(AlO)OH_4]^-$ etc. make excellent precursors for geopolymers due to their naturally occurring structure and stoichiometry. Ideal candidates for geopolymerzation contain a Si:Al ratio between 2-4 (this ratio can be artificially increased during synthesis if the base aluminosilicate source is lacking silicon content by use of an alkaline silicate solution).

Next, an aqueous alkaline solution (or an aqueous alkaline silicate solution if extra silicon is needed to balance the Si:Al ratio) is added to the aluminosilicate source. Upon mixing, the aluminosilicate source is completely dissociated by the alkaline solution into

common Si and Al species, i.e. monomers or oligomers. The species formed during dissociation can be seen in Figure 4b. After dissociation, the species begin to chain together monomerically by forming into –Al-O-Si- or –Si-O-Si- bonds during a polycondensation process in which excess water is released, as seen in Figure 4c.

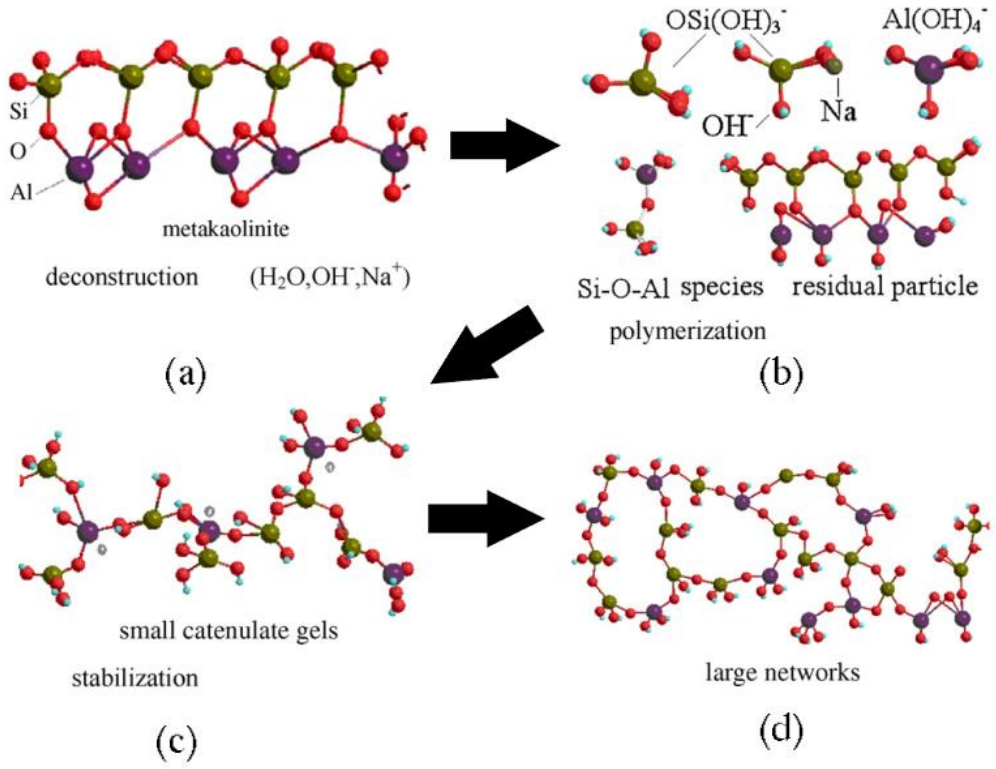

Figure 4: Illustration of geopolymerization process [7]

The aluminosilicate chains continue to grow during the polycondensation process. During this process various monomeric, oligomeric, and polymeric units continue to produce chains and crosslink until an amorphous gel with a complex 3D structure is formed, as is illustrated in Figure 4d**.** To accelerate curing of the initial gel, it is usually

exposed to a temperature of 60-80 ^{o}C. The geopolymers continue to polycondensate and lose water mass until they are fully cured, which takes approximately 21 days at room temperature [28].

The final geopolymer structure can be described as an amorphous, 3-D framework of corner-sharing $[SiO_4]^{4-}$ and $[AlO_2]^{5-}$ tetrahedra in IV-fold coordination [29], where the IV-coordinated aluminum present in the structure differentiates a geopolymer from other poly-aluminosilicate materials. The negatively charged Al ions in the geopolymer are balanced by residual alkali cations which remain loosely incorporated into the geopolymer structure. These cations are hydrophilic and retain some water in the geopolymer structure after curing [12, 30].

After completion of the curing process, a rigid, aluminosilicate polymer with an amorphous, complex, 3D network structure, referred to as geopolymer, is formed.

1.4 Applications of Geopolymers

While geopolymers possess similar physical characteristics to Portland cement that make them an excellent alternative for concrete in traditional construction applications, they also possess many other properties that can be utilized in other industries and applications.

1.4.1 Thermal Protection Applications

Geopolymers have inherently low thermal conductivity due to their chemistry and open framework structure. Their conductivity can be lowered even further by introducing porosity to their structure by introducing excess water to the geopolymer mixture. The geopolymer can also be foamed while in gel phase, creating a very lightweight porous material [31]. These traits make geopolymers a prime candidate for insulation applications where an inexpensive, durable material with low thermal conductivity is needed.

Many researchers have conducted tests on the thermal conductivity of geopolymers. Duxson et. al. [32] measured the thermal conductivity of Geopolymers and found it to lie between 0.2 and 0.6 w/m.K, depending on their chemistry and structure. This falls well below range of traditional construction materials, especially concrete (K = 1.6 – 1.9 w/m.k) [33]. Geopolymer based insulations have successfully replaced several types of insulation in a variety of applications, but have the potential to excel in industrial casting environments as a refractory cement. For example, ceramic fiber reinforced Geopolymer composites do not experience the same level of crack propagation as alternative refractory cements because their stiffness increases with temperature rises, in addition to the fiber reinforcement preventing excessive crack propagation leading to failure [34].

Geopolymer foams are the latest in aluminosilicate based thermal protection. As studied by Zhang et. al., these foams provide an economic and environmentally friendly material that is simple to produce and can be used for a variety of applications. Zhang suggests

these foams can either be directly applied to existing structures to add thermal insulation and structural reinforcement, or cast into blocks to create a portable construction material [31].

1.4.2 Fireproofing Applications

Geopolymers are also considered to be an ideal candidate for both fireproof materials and coatings due to a variety of factors. First, as discussed above, they possess low thermal conductivity. This is beneficial, especially in the application of thermal barrier coatings, as it prevents heat transfer to the substrate. Second, geopolymers are able to be synthesized into a liquid ‘gel’ before curing, allowing them to be applied with methods such as rolling, brushing, or even spraying [35, 36]. Many traditional fireproofing materials are distributed in rolls or sheets, preventing uniform coating of complex geometries. Geopolymer paint could present an inexpensive solution to fireproof coatings for many applications. An example of geopolymer based fire retardant coating being tested can be seen in Figure 5.

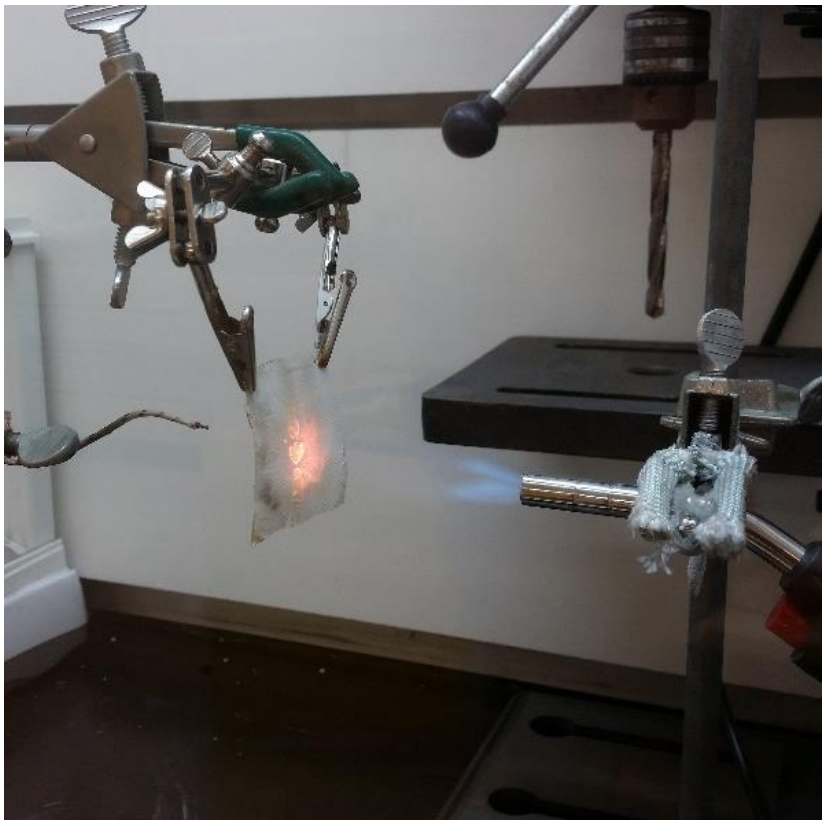

Figure 5: Flame testing of a fire retardant geopolymer coating

Bakharev et. al. conducted a study on the thermal behavior of fly ash based geopolymers exposed to temperatures similar to those found in aggressive fires. They found that certain geopolymer compositions remain amorphous at temperatures up to 1200 ^{o}C rather than breaking down into alkaline feldspars as many other aluminosilicates do. Furthermore, these samples exhibited increased compressive strength upon heating in contrast to many materials which are susceptible to thermal creep at elevated temperatures [37].

One particular concern of concrete structures is their tendency to spall under thermal stresses. The concrete absorbs water, which upon application of heat turns to steam and breaks off large chunks of the concrete due to internal stresses. Spalling is a rather common concern when designing large structures made of concrete, and structural columns and other vertical supports loaded in compression have the potential to explode when exposed to fire due to their particularly low permeability and high brittleness [38]. Due to their internal cross linking, geopolymers tend to resist spalling much more than traditional Portland cement based concretes while maintaining equal or higher compressive strength.

1.4.3 Chemical Resistance

Another environment where concrete is not a viable construction material is in acidic environments. Strong acids, such as sulfuric or hydrochloric acid, dissolve the Portland cement component of traditional concrete rendering it unstable. Geopolymer based materials have much better acid resistance than concrete, even in long term exposures. Tests in which geopolymer samples have been submerged in strong acids for long periods of time show minimum (if any) mass loss, versus complete dissolution for Portland cement based concrete [39, 40]. In fact, recent research has shown that exposure to strong acids does not alter the geopolymer microstructure significantly [41]. It has been hypothesized that the internal aluminosilicate polymer structure inhibits acid erosion.

Due to their chemistry, geopolymers are naturally resistant to highly basic environments due to the free OH^- groups built into their structure. These properties make geopolymers a natural pH stabilizer, and they have been used with some success in this application in research [42].

1.5 Objectives of the Research Work

The importance of this research work presented here stems from the ability to create a product that is extremely beneficial to the industry. Historically, bonding of ceramic to metal has been done with using either adhesives or brazing. In order to make the ceramic adhere to the metal, the ceramic is first infiltrated with a metallic braze. Next, the metallic component is attached and soldered to the infiltrated ceramic component. This method is preferred when an electrical or thermal bond is required. Problems arise at high temperatures, as solders and brazes that are capable of being applied usually melt at temperatures below 500 ^oC. In addition, the joint is not thermally or electrically isolated and susceptible to corrosion [43].

The most widely used current methods for adhesion rely on polymer based adhesives. Many of these products are general purpose adhesives that will work with metals and ceramics. For example, cyocrylanate (CA) glue can be used to bond stainless steel or titanium to glass, but has a very low shear strength and an even lower melting point. In addition, polymer based adhesives usually require surface preparation, which usually

requires either physically or chemically roughing the surface in order to give the adhesive a method to penetrate the substrate [44-46].

Other adhesives exist that have much higher working temperatures. For example some alumina based adhesives are capable of withstanding working temperatures of up to 4000 ^{o}F. These products are excellent for ceramic or refractory adhesion, but are not ideal for adhering metallic substrates together as they do not penetrate the metallic surface that results in a very weak bond. Other factors include high cost and low compressive strength (due to high porosity) [47].

Geopolymer-based adhesives fill in niche in the currently available adhesive lineup for a product that is capable of bonding metallic and ceramic substrates with low thermal conductivity, high corrosion resistance, and low cost.

2 LITERATURE REVIEW

In order for Geopolymer based cements to be a suitable adhesive for metallic substrates at high temperatures, they must outperform current adhesives in their mechanical strength, chemical adherence to metallic substrates, thermal resistance, and their chemical resistance in aggressive environments. Many studies have been performed on these topics and some of the results have been summarized in the following sections.

2.1 Mechanical Properties of Geopolymers

It is critical for an adhesive to be able to bear a high tensile load. Research has shown that Geopolymers possess a relatively low tensile strength compared to most metals, but their relative tensile strength is quite high compared to many ceramics. Buchwald et. al showed that in both slag and metakaolin based geopolymers, the tensile strength is almost always directly proportional to the compressive strength, with an average range of tensile strengths between 7 to 12 MPa [14]. For comparison, most polymer based glues, with proper surface treatment, possess a tensile strength in the range of 5 to 30 MPa [48] [49]. Several other studies have shown similar tensile results to Buchwald's in other baseline studies where the geopolymer chemistry has been altered [4, 50-52]. Dombrowski et. al determined that an addition of Calcium Hydroxide to the geopolymer gel actually increase the tensile strength of geopolymer cements at elevated temperatures by a small percentage by forming an amount of feldspar in the geopolymer matrix [24]. Analyzing these previous results show that geopolymer matrix is strong enough in

tension to be a feasible adhesive, comparable in strength to polymer based adhesives. In addition, the research shows that both metakaolin and fly ash based geopolymers possess high enough tensile strength to be feasible adhesives, and the additions of small impurities to the initial reagents or the geopolymer gels does not cause catastrophic degradation of the tensile strength. All of these conclusions support feasibility of using geopolymer gel as an adhesive.

As the most researched component in geopolymer research is the ability to create environmentally friendly alternatives for concrete, a great number of studies have been reported on Geopolymer compressive strength and performance with and without common aggregates in many different compositions. One of the most influential studies on this research work was the work conducted by Lizcano et. al on the effect of water content on geopolymer' s properties. Lizcano et al. showed that while previous methods of geopolymer synthesis simply added water to the geopolymer gel to obtain a workable viscosity for casting, the water content in the geopolymer gel possesses a strong influence on the final porosity of the geopolymer. As the porosity increases, the geopolymer's compressive strength decreases [12]. Westwick et. al showed that when higher water ratios are used during the production of geopolymer gel, increasing the amount of alkali used during synthesis can lead to higher compressive strength while an excessive amount of alkali leads to a lower compressive strength. This is theorized to be caused by additional alkali allowing charge balancing in the geopolymer structure when high amounts of water leach some of the alkali material, while an excessive amount of alkali material acts as a 'chain terminator', causing the polycondensation process to stop

prematurely and preventing some crosslinking. When geopolymers are created with optimized chemical and water ratios, their compressive strength can exceed 100 MPa, vastly exceeding the compressive strength of most Portland cements [23]. While compressive strength is not critical for this work, these research works show that geopolymers will fail in tension or shear modes before compressive modes, allowing us to eliminate compressive testing from the experiment design.

2.2 Adhesion of Geopolymers to Various Substrates

In order to be a viable adhesive, geopolymers must be capable of adhering to substrates via mechanical interlocking or chemical bonding. Mechanical interaction between geopolymer and the underlying substrate has been studied in depth by many researchers, as geopolymers show promise to make thermally resistant coatings on metallic substrates. Temuujin et. al has conducted several experiments involving the coating and adhesion of mild steel substrates with geopolymer adhesive[35, 36, 53]. In an early test performed with sodium cured fly ash based geopolymers, it was shown that geopolymers were capable of coating a mild steel substrate with the primary factor of effectiveness being the geopolymer composition, most importantly the water content. The results were promising, with a tensile strength of 3.5 MPa being attained. More testing was shown to reveal a high water content leads to a low thickness coating while a lower water content provides a thicker coating, but is more susceptible to cracking during curing. After a certain thickness the geopolymer ceases to effectively adhere to the substrate, theorized

to result from warping during curing [36]. In a later test a sodium silicate/metakaolin based geopolymer was used. The geopolymer was tested to determine its water solubility after testing, with results ranging from 12 to 35 percent leaching, depending on the initial concentration. In addition, the coated specimens were exposed to elevated temperatures for short periods of time. The geopolymer adhesive showed a 3% thermal expansion relative to the substrate after heating at 800 ^{o}C for 1 hour [35]. These results are supported by other research data, showing geopolymer coatings have relatively high tensile strength and make excellent coatings when processed properly [53].

Latella et. al has shown that geopolymer based adhesive is capable of bonding glass and steel substrates effectively with both fly ash and metakaolin based compositions [54]. In addition, Ueng et. al has determined that geopolymer based adhesive excels in the joining of different cement mortars under conditions where they would normally be unable to bind to each other [55]. Finally an important result from De Barros et. al shows us that the surface preparation of the substrate has little to no effect on the bonding strength of the interface [56]. These results show great promise to the experiment, as geopolymers have been successfully bonded to metallic substrates. The fact that surface preparation does not significantly increase tensile strength supports the theory that an underlying chemical bond is present in the geopolymer-substrate interface.

2.3 Chemical Bonding of Aluminosilicate to Metal Oxide Layers

Aside from mechanical strength, another critically important facet to analyze is the ability for geopolymer based adhesive to chemically bond to the substrate material. While little research to date has been conducted on the adhesive properties of geopolymer cements, many studies have been conducted in the field of dentistry on the chemical bonding of silicon based gels and adhesives to titanium substrates, as many dental implants are made of titanium. Adachi et. al and Ozcan et. al have both analyzed the adhesive strength of silicon based gels to titanium via oxide adherence. Oxide adherence allows silicon and titanium to bond through a shared oxygen atom in the oxide layer of titanium, creating a Si-O-Ti bond. These bonds have relatively high strength and are created spontaneously when curing a silica-based adhesive [57, 58]. Wang et. al also performed experiments on oxide adhesion using a silicon nitride coating on titanium, allowing a common alumina based porcelain to bond to a titanium substrate chemically but allowing oxygen diffusion during the firing process [59]. These studies dictate that is it possible for a silicon atom to bond to the oxide layer of a metallic substrate without the addition of any additional energy addition to the system or any special preparation work. It also shows that Si-O-Ti bonds are a reliable mechanical bond capable of adherence to a titanium substrate. The titanium oxide adherence could theoretically be carried over to any metallic substrate with a nonreactive oxide layer, including aluminum oxide, chromium oxide (in stainless steel), and even possibly iron oxide. These results are optimistic for the purposes of a geopolymer based adhesive; chemical adhesion potential shows geopolymer gel, which is primarily constructed of

silicon, aluminum, and oxygen, has a high chance of creating oxygen adherence to a metallic substrate with an oxide layer.

2.4 Thermal Resistance of Geopolymers

For use in an industrial environment, an adhesive must possess high thermal resistance. The thermal properties of geopolymers have been widely studied due to their inherently low thermal conductivity and use in possible insulation applications. Barbosa and MacKenzie showed that geopolymers continue to possess their basic Al-O-Si amorphous crosslinked structure until their melting point between 1200 and 1300 ^{o}C. They also showed that while the geopolymer samples lost their excess water at 200 ^{o}C, they did not shrink excessively. In addition, at higher temperatures the geopolymers showed very little thermal expansion, making them ideal for high temperature applications [60]. Bakharev et. al showed that geopolymers possess excellent mechanical properties up to temperatures exceeding 1000 ^{o}C before they begin to degrade. However the geopolymer itself remained amorphous and did not begin conversion to feldspar and thus break down the cross linked matrix [37]. Since the geopolymer does not shrink when exposed to high heat and does not have an excessively high thermal expansion coefficient, it can be assumed the metallic substrate will expand at a higher rate than the geopolymer based adhesive. This would prevent the adhesive from delaminating from the substrate at elevated temperatures if the thermal expansion coefficient of the geopolymer was higher

than that of the substrate. Instead, the geopolymer adhesive may simply crack between substrates, but still retain a chemical bond with the substrate.

3 EXPERIMENTAL METHOD

3.1 Substrate Preparation

Samples for this experiment were prepared in accordance with ASTM D897-08 for tensile specimens and ASTM 1002-10 for shear specimens. Small sample coupons were also created for microscopy analysis and to heat treat to determine the effect of high temperature to the geopolymer adhesive.

The tensile specimens were created using a modified ¾ - 10 bolt made from grade 2 pure titanium or 316 stainless steel. The bolt was placed thread first into a collet on a manual toolroom lathe. First, the front head of the bolt was machined flat to remove any dents, lettering, or other defects on the surface. A low feed rate was used on the lathe to avoid any grooving due to high feed speeds. Next, the side of the bolt was turned down to a diameter of 1.000 inches, with a tolerance of ±0.0005 inches. This allowed extremely accurate calculation of the surface area the adhesive is applied to, resulting in reliable calculations of the tensile strength. The tensile samples before processing can be seen in Figure 6.

Figure 6: Tensile test specimen before adhesion

The shear specimens were prepared using different tooling for each material. Due to the relatively high cost of the titanium plate used, a Computer Numerically Controlled (CNC) Mitsubishi FA Series wire Electrical Discharge Machine (EDM) was used to create the ¾ inch wide strips of titanium used for shear testing. This was done primarily to minimize kerf waste and to provide the maximum number of samples from the titanium stock. Upon receipt from the wire EDM, the specimens were extremely dirty from the machine. They were cleaned using 600 grit sandpaper and ethyl alcohol before being prepared for testing. The specimens were finally scored ¾ inch from the end to aid in the measurement during the creation of the lap shear specimens.

The stainless steel strips used in shear testing were cut from a larger plate and therefore did not need wire EDM. A South Bend Lathe Company SB1019 horizontal band saw was used to cut the strips approximately 7/8 inches wide. Next, the strips were squared

on a Bridgeport vertical milling machine using a ½ inch carbide end mill. Finally, a jig was created to allow the strips to be held vertically and milled to exactly ¾ inch wide using the carbide end mill. The specimens were finally scored ¾ inch from the end to aid in the measurement during the creation of the lap shear specimens. The Titanium and Stainless Steel shear specimens before processing can be seen in Figure 7.

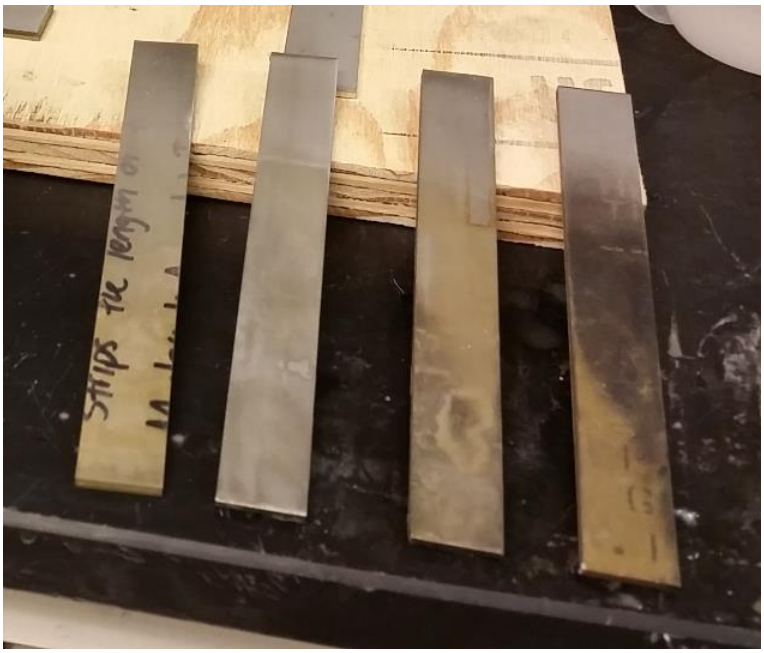

Figure 7: Shear test specimens before adhesion

The ¾ inch square heat treatment coupons were cut with wire EDM in a manner similar to the titanium shear specimens. Upon receipt they were cleaned with 1000 grit sandpaper and ethyl alcohol before preparation for testing. The heat specimens as well as the plate they were cut from can be seen in Figure 8.

Figure 8: Heat treatment specimens before adhesion

3.2 Geopolymer Gel Synthesis

Geopolymer gel is formed of a combination of commonly found raw ingredients. While geopolymers are capable of being synthesized from fly ash, it is easier to control the purity, reaction rate, and the resultant properties when they are synthesized from metakaolin clay. In this study we use metakaolin (METAMAX, BSF Catalysts Ltd., NJ) and fumed silica (Alfa Aesar, MA) together with NaOH (Alfa Aesar, MA) or KOH (Alfa Aesar, MA) alkali activators and deionized water to prepare geopolymer gels. First, the quantities of material needed to prepare geopolymers with different compositions, i.e. with different Si/Al and $(SiO_2+AlO_2)/H_2O$ rations were measured. In all samples, Na/Al or K/Al ratio was kept constant and equal to 1. Geopolymers with different composition

were labeled in this study as X-Y-Z, where X is akali activator (Na or K), Y is Si/Al ratio and Z is $(SiO_2+AlO_2)/H_2O$ ratio.

The water is measured and placed into a borosilicate glass beaker. A stir bar is added, and the beaker is placed onto a stir plate. NaOH or KOH is then weighed and slowly added to the water to form an alkaline solution. The solution is kept covered during mixing to prevent water vapor from escaping the solution or carbon dioxide from entering it as the acidity of carbon dioxide can neutralize the OH- ions and cause poor dissolution of the silica in the next step or even incomplete geopolymerization. This solution must be well mixed before continuing, and is stirred for 2 to 4 hours depending on the quantity of alkali used.

The alkaline solution is then processed into an alkaline silicate solution. Fumed silica is weighed and added slowly to the alkali solution as it dissolves. Adding the silica too quickly results in the alkali solution being wicked into the fumed silica before the silica can be dissociated, and can result in failure of the synthesis. Adding the silica usually takes between 1 to 2 hours. Upon completion, the alkaline silicate solution must be well mixed (usually for 24 or more hours) before continuing.

Finally, the geopolymer gel is created by adding the silicate solution to the metakaolin clay. The clay is weighed and added to the stir chamber of a vacuum mixer (Whipmix, KY). The well-mixed silicate solution is also added to the stir chamber. The mixture is stirred in a vacuum for 5 minutes to ensure all of the metakaolin clay has been dissolved. In the event of an extremely viscous mixture which prevents the paddle in the mixer

from operating, the stir chamber is removed and mixed manually until the viscosity decreases enough to allow the vacuum mixer to function properly.

Upon completion of mixing, the geopolymer gel is stored in syringes for short term storage and easy application. The gel remains viable for an approximate 1 hour period, upon which it has sufficiently polycondensated and is too viscous to extrude properly. A syringe of geopolymer gel ready for application can be seen in Figure 9.

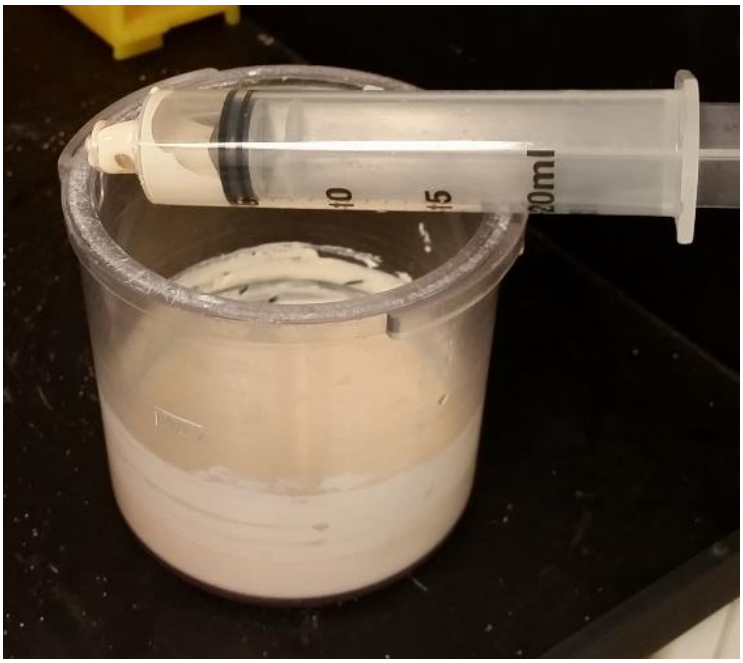

Figure 9: Syringe of geopolymer gel adhesive ready to be applied

3.3 Geopolymer Gel Wetability

In order to determine ideal geopolymer gel compositions to use as adhesives, a wettability test was performed to measure the contact angle and thickness of the geopolymer gel when applied to the metallic substrate. Approximately 0.5 mL of several

types of geopolymer gel was applied to a polished strip of each of the metallic substrates that were used in this work (titanium and stainless steel). The specimens were then photographed from the side to determine the variance in contact angle as well as the adhesive layer thickness. The strips were then placed in a convection oven to cure to determine the degree of thermal expansion cracking.

3.4 Substrate Surface Preparation

The adhesion test substrates are prepared in several different ways. However, before any preparation work is started all of the substrates are thoroughly washed with distilled water to prevent impurities from being introduced from external sources.

For the tensile 'bolt' specimens, a lathe was used to remove approximately 0.005 inches off the end of the bolt to remove cured geopolymer from previous tests. Next, the edges of the bolt are chamfered at a 45 degree angle approximately 0.002 inches to remove the burrs resultant from machining. The mating heads of the bolts are then sanded and polished using 200 then 400 grit sandpaper. Finally, the specimens are thoroughly cleaned with deionized water, followed by ethyl alcohol.

The shear specimens are prepared similarly to the way the tensile specimens are prepared. First, the residual geopolymer from previous tests is removed with a putty knife and 200 grit sandpaper. A visual inspection confirms the specimen is free of previous geopolymer material or large flaws before it is reused. The specimen is then

sanded with 400 grit sandpaper and cleaned with deionized water and ethyl alcohol. Several iterations of the tensile and shear specimens were conducted with a highly polished surface in order to minimize the mechanical interaction between the geopolymer and substrate. These specimens were prepared the same as the tensile and shear specimens above, but with a polish regimen of 150-400-600-1000-1500 grit silicon carbide sandpaper, followed by 12-6-3 μm diamond polishing paste. The final surface was lightly buffed with a soft cloth and ethanol, leaving a mirror finish that can be seen in Figure 10.

Figure 10: Mirror polished tensile test specimens before adhesion

Since they are only used once, the heat treatment coupons do not need to have excess geopolymer residue removed from them between tests. They are lightly sanded with 400 grit sandpaper and cleaned with water and ethyl alcohol before adhesion.

3.5 Adhesion of Substrate with Geopolymer Gel

3.5.1 Tensile Specimens

Once the tensile specimens' surfaces were prepared, they were loaded into a custom created fixture to ensure proper adhesion. The bottom bolts were first loaded to the bottom plate and secured, using a ¾-10 nut. Next, the top bolts were threaded through the aluminum plate. Finally, the top plate was secured to the bottom plate using two precision machined risers and screws. The specimens can be seen in the jig prior to curing in Figure 11.

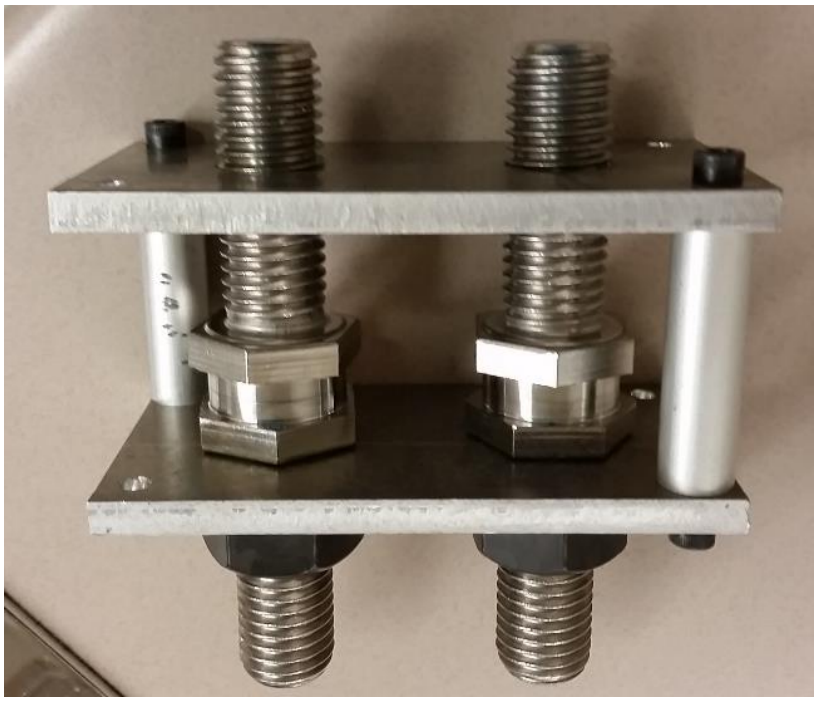

Figure 11: Tensile test specimens in alignment jig during adhesion

Once the fixture was assembled, a large drop of geopolymer gel (approx. 0.5mL) was applied to the head of the bottom bolt. The top bolt was then threaded down until it was in contact with the bottom bolt, squeezing the excess geopolymer paste out the sides. The thickness of the adhesive layer and the contact pressure could be controlled through how far the top bolts were threaded through the aluminum plate. For this set of tests, the bolt was turned finger tight, resulting in a contact force of approximately 20N and a geopolymer adhesive layer approximately 20μm thick.

3.5.2 Shear Specimens

Shear specimens were prepared with a jig that allowed both plates to be positioned in a perfectly straight line. After the specimens' surfaces were prepared, strips of wax paper were cut ¾ inch wide and placed to the side. A strip of wax paper was laid into the jig, followed by a full metal strip on one side of the jig, and a piece of metal scrap on the other side of the jig. The metal scrap allowed the second strip to sit level on top of the first strip. Next, a syringe was used to dispense approximately 0.25mL of geopolymer gel onto the end of the first plate. A second plate was then aligned with the scribe mark and placed on top of the first plate to create a shear lap joint. Upon later inspection, the weight of the metal alone caused the thickness of the geopolymer paste to vary between 50μm and 200μm. To rectify this, the specimens were recreated, but with a 2kg weight resting on them during curing. This allowed the adhesive layer to remain constant for all samples, with a thickness of approximately 30μm.

Upon completion of the single shear specimen, a second piece of scrap metal was placed opposite to the top plate to create a level surface for the next specimens to sit on. Another piece of wax paper was added on top of the specimen, and the process was repeated until all shear specimens had been assembled.

3.5.3 Specimens for Thermal Treatment

After surface preparation, specimens for thermal treatment were prepared by applying a small drop (approximately 0.25mL) of geopolymer gel to the bottom substrate, followed by the top substrate. Upon completion, the samples were stacked in a v-shaped channel to prevent them from turning or sliding during curing. Samples were separated using small squares of wax paper. The assembled heat treatment coupons can be seen in Figure 12.

Figure 12: Thermal treatment coupons in fixture during curing

3.6 Controlled Curing

All samples were cured in a low temperature convection oven at 65 degrees Celsius for 24 hours in sealed containers. Following the initial curing, the samples were left to age at room temperature between 4 and 7 days, allowing excess water in the samples to dissipate.

3.7 High Temperature Treatment

Several samples were exposed to high temperatures to determine how well the adhesive performed in an elevated temperature environment. The oven was first calibrated using a

J-type thermocouple. Upon reaching the desired temperature, samples were placed in the oven and left for 24 hours. Upon removal, the samples were left at room temperature for 24 hours to stabilize prior to testing or analysis.

3.8 Sectioned Samples for Microscopy

Several specimens from each batch were created for microscopy following the same techniques as listed above. These specimens, once cured and aged, were carefully cast in Buehler EpoxiCure 2 Resin and sectioned using a Buehler Isomet 1000 precision sectioning cutter. The half specimens cut surface were then polished on an Allied M-Prep 5 Polisher using silicon carbide sandpaper grits 300, 400, 1000, and 1500. This initial sanding was followed by buffing with 12micron, 6micron, 3micron and 1micron diamond polishing compound to achieve the smoothest possible surface finish. One of the half samples which was to be used for Optical Microscopy (OM) and Scanning Electron Microscopy (SEM) and analysis was sputter coated with a 5um layer of platinum after being left to cure in a low temperature convection for 3 days to remove residual water.

3.9 Testing

3.9.1 Microscopy

All optical microscopy analysis was performed with a Keyence VHX series digital microscope. In order to avoid localized singularities, multiple exposures were taken of the specimen in slightly different locations with varied brightness and contrast settings. SEM was performed using a JEOL JSM series Scanning Electron Microscope (SEM) equipped with Energy-dispersive Spectroscopy (EDS) detectors for analyzing chemical composition.

3.9.2 Tensile Testing

Tensile testing was performed on an Instron 5900 series tensile testing frame with a 5kN load cell attached. Samples were attached to the frame via a set of custom machined fixtures that allowed the ¾-10 bolts to be attach to the pin mount of the frame. While threading the bolts into the fixtures, great care was taken not to apply any torsion, bending or shear loading to the substrate-adhesive interface. In addition, no preload was applied to the samples before the start of the test.

Figure 13: Tensile test specimen after tensile failure

Once the samples were attached to the frame, they were loaded with a constant extension rate of 0.05 in/s. Upon failure, specimens were removed from the fixture to be analyzed further. The force and extension at break were recorded and the sample was set aside to be analyzed at a later time. An example of a tensile specimen after failure can be seen in Figure 13.

3.9.3 Shear Testing

Shear specimens were also tested on an Instron 5900 series tensile testing frame with a 5kN load cell. Samples were attached to the frame via Instron self-tightening grips. In order to prevent bending moments from developing during testing, the samples were shimmed on both sides until they were perfectly symmetrical in the grips. Once again, great care was taken to avoid applying shear, tensile, torsion, or bending loads to the interface prior to the test.

The samples were subjected to the same extension rate as the tensile samples of 0.05 in/s. Due to the lack of a pin connection, these samples did not need to be pre-loaded and usually had a small amount of tensile force already applied before the test began.

Upon failure the specimens were removed from the grips and set aside to be analyzed further at a later time. The force and extension at break were also recorded for each sample identifier. An example of a shear test after failure can be seen in Figure 14.

Figure 14: Shear test specimen after shear failure

3.9.4 Heat Treated Tensile Specimens

Heat treated tensile specimens were tested with the same parameters as tensile specimens with the addition of a heating cycle prior to testing. For all samples tested in this work, the heating cycle prior to tensile testing was 500 °C.

4 RESULTS AND DISCUSSION

4.1 Surface Wettability

In order to determine the most optimal geopolymer compositions to test, surface wettability tests were performed. Geopolymer gel was carefully dropped onto a polished strip of each substrate metal. The strips were then photographed from the side to determine the approximate contact angle. A photo of the wettability test before curing can be seen in Figure 15.

Figure 15: Surface wettability on stainless steel and titanium substrates

Analysis of the contact angle revealed geopolymer compositions with high water content exhibited the highest contact angle, while compositions with high silicon content possessed the lowest contact angle. The substrate strips were covered and placed in a convection oven to cure for 24 hours to determine the effects of water loss. The cured samples can be seen in Figure 16.

Figure 16: Wettability samples after 24 hours curing at 70 °C

After curing, the geopolymer composition ratios of K-3-2 and K-3-4 were chosen for synthesis. The K-3-2 ratio was chosen due to its lack of cracking during curing, and the K-3-4 composition was chosen due to its high contact angle during its gel phase. It is unclear why the compositions with high Si/Al ratios exhibited such extensive cracking during curing.

4.2 Adhesive Gap

4.2.1 Optical Microscopy

After being sectioned, the specimens were analyzed using optical microscopy. Analysis at the magnification of 500 and 1000 times was used to determine the overall thickness of the adhesive gap. The adhesive gap width for a K-3-2 geopolymer based adhesive on a stainless steel substrate can be seen in Figure 17 to have a gap thickness of

approximately 60 um, while the same K-3-2 geopolymer adhesive when applied to a Titanium substrate gives a thickness of approximately 80 um as seen in Figure 18. This discrepancy in adhesive thickness could be caused from a variety of sources, but is most likely due to the higher pressure applied by the heavier stainless steel top substrate, as in this test no force regulation was used during the adhering process.

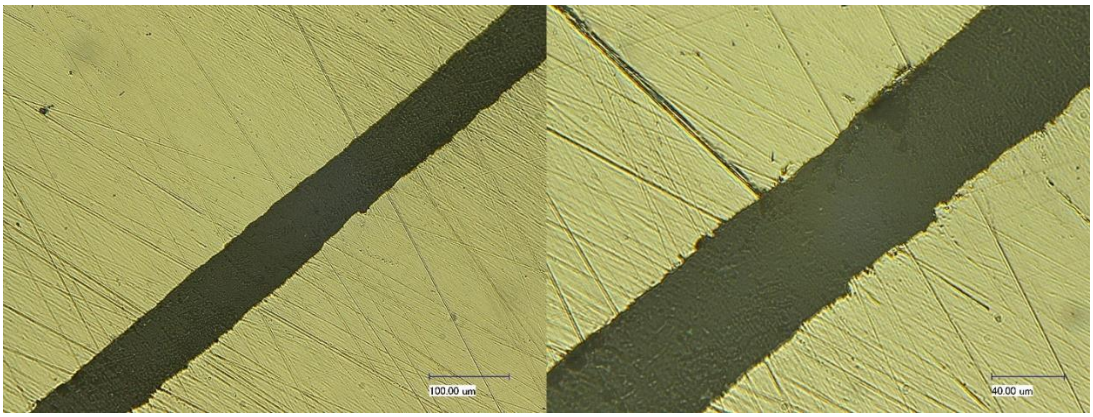

Figure 17: K-3-2 stainless steel adhesive gap

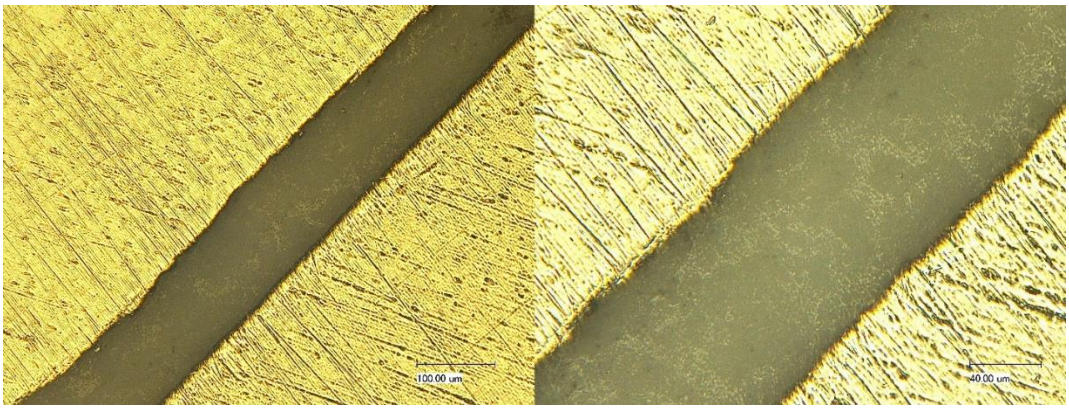

Figure 18: K-3-2 titanium adhesive gap

An additional set of specimens created with a less viscous adhesive, K-3-4 was also analyzed. K-3-4 based geopolymer gel has twice the water content as K-3-2 geopolymer gel and therefore is much less viscous. The lower viscosity adhesive led to smaller adhesive gaps. The gap in the K-3-4 Stainless Steel specimens was on the order of 30 um as seen in Figure 19, while Figure 20 shows the gap for K-3-4 tensile specimens to be approximately 60 um. It should be noted that the leading surfaces of the titanium substrate used in this particular experiment were possibly damaged during sectioning, leaving a strange pattern in the photos that is non-indicative of the actual surface (the sample was sectioned using a different sectioning saw that was much less sharp than the saw used to section all of the other specimens in this work).

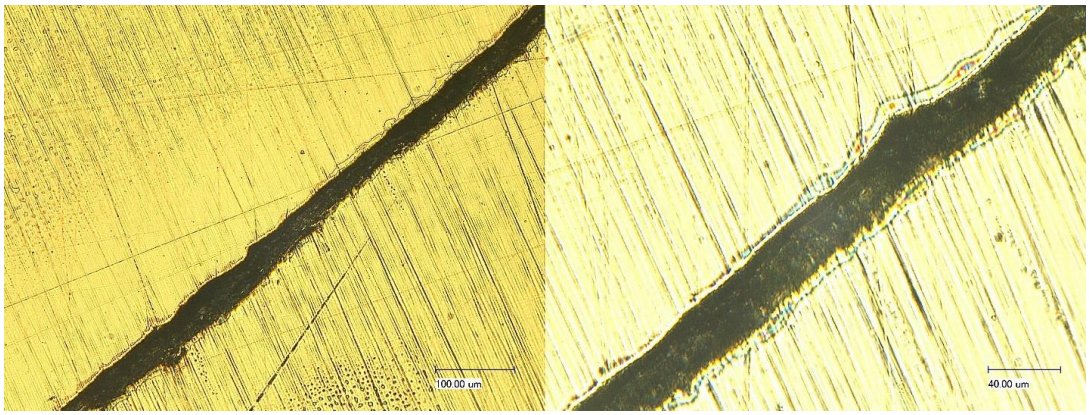

Figure 19: K-3-4 stainless steel adhesive gap

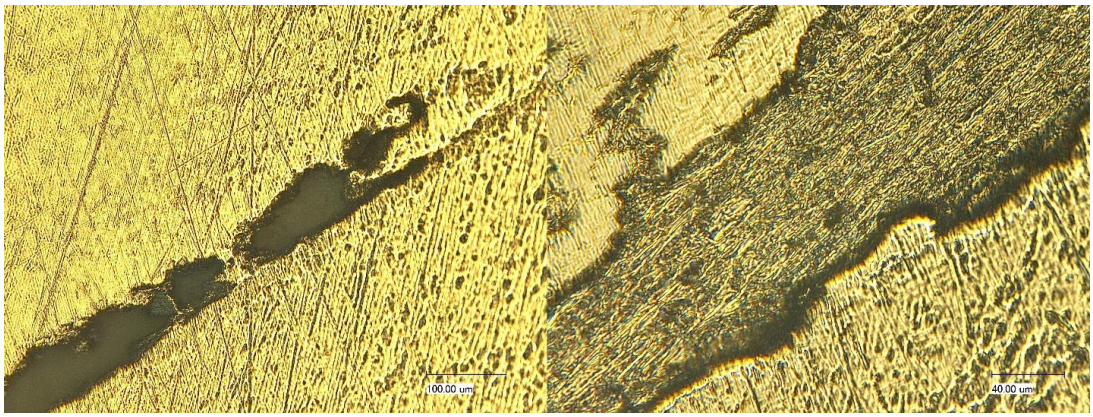

Figure 20: K-3-4 titanium adhesive gap

4.2.2 Electron Microscopy

Electron microscopy on platinum sputter coated sectioned samples reveals similar results for adhesive gap thickness to the optical microscopy results. Figure 21 depicts an adhesive gap for the K-3-2 Stainless Steel specimen of approximately 60um. However, Figure 22 shows a much higher thickness in the adhesive gap for the K-3-2 Titanium of approximately 150 um. These results show how unreliable adhesion without a pressure can be.

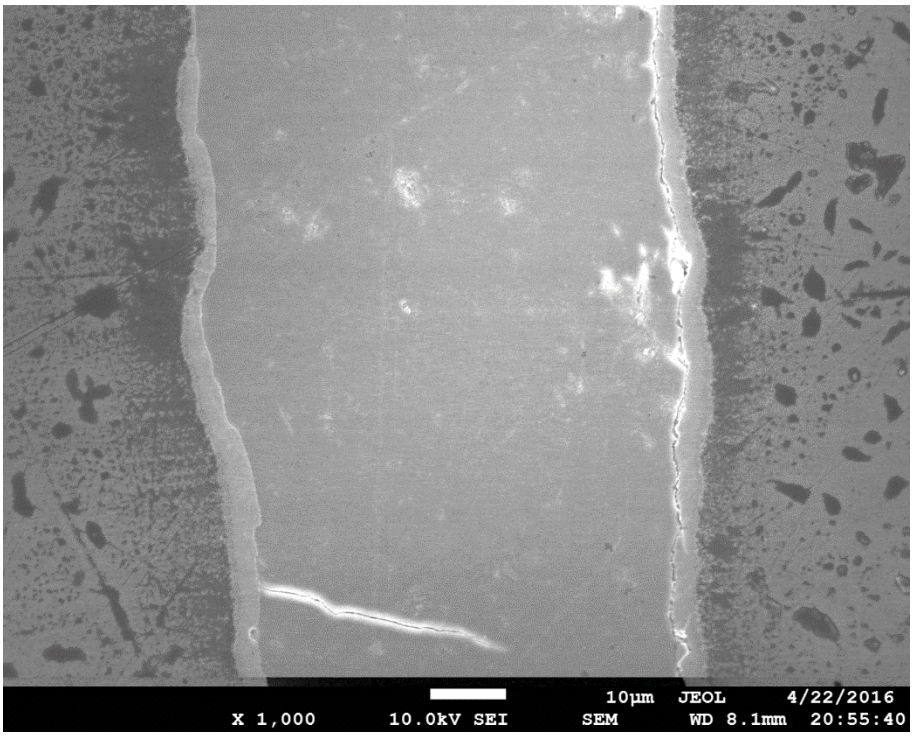

Figure 21: K-3-2 stainless steel adhesive gap

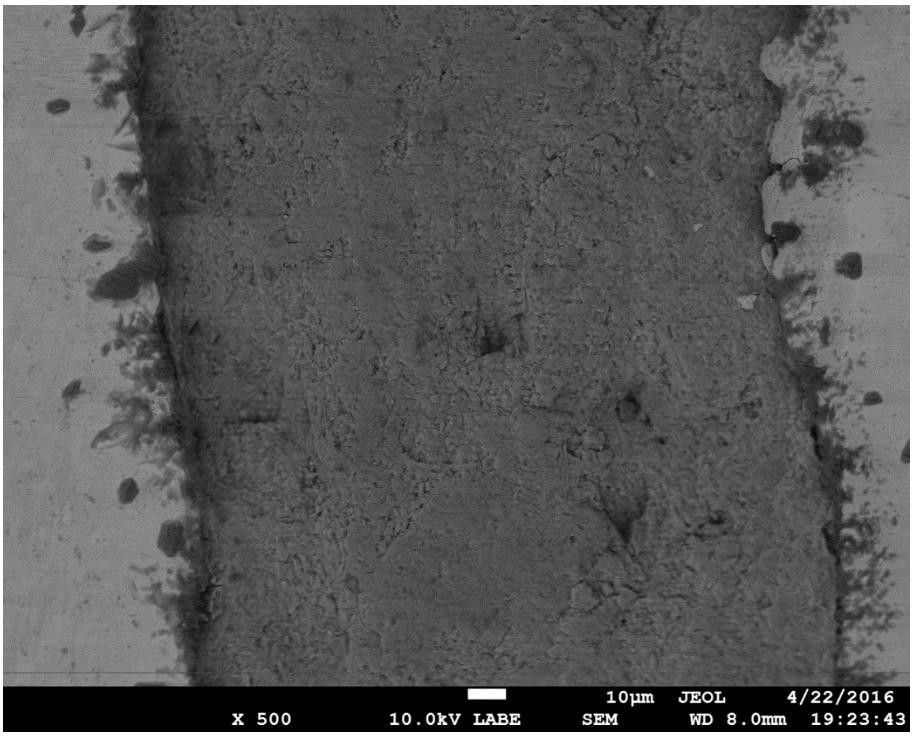

Figure 22: K-3-2 titanium adhesive gap

4.2.3 Reduction of Gap

In order to create more consistent samples in addition to reducing the thickness of the adhesive gap, some specimens were put under pressure during curing. This was done one of two ways: by adding a 2kg weight to the tops of the specimens during curing or by using a clamp or jig to hold the specimen under pressure during curing (as seen in Figure

23). The results of the thicknesses of the adhesive layer can be seen in Table 1 and Figure 24.

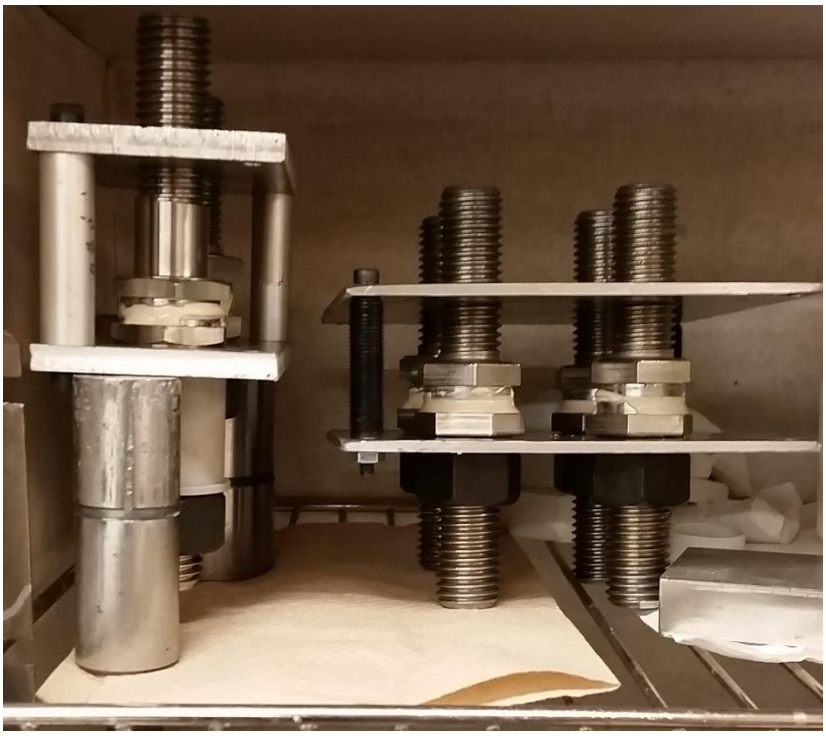

Figure 23: Clamping jigs used for applying pressure to tensile specimens during curing

Table 1: Minimum and maximum observed adhesive gap for various geopolymer gel compositions and fixturing methods

Treatment	Substrate	Composition	Min Thickness (um)	Max Thickness (um)
None	Stainless Steel	K-3-2	45	70
		K-3-4	20	65
	Titanium	K-3-2	75	160
		K-3-4	45	90
Weighted (2kg)	Stainless Steel	K-3-2	20	45
		K-3-4	10	35
	Titanium	K-3-2	30	80
		K-3-4	25	55
Clamped (2kg)	Stainless Steel	K-3-2	25	65
		K-3-4	20	50
	Titanium	K-3-2	45	85
		K-3-4	30	60

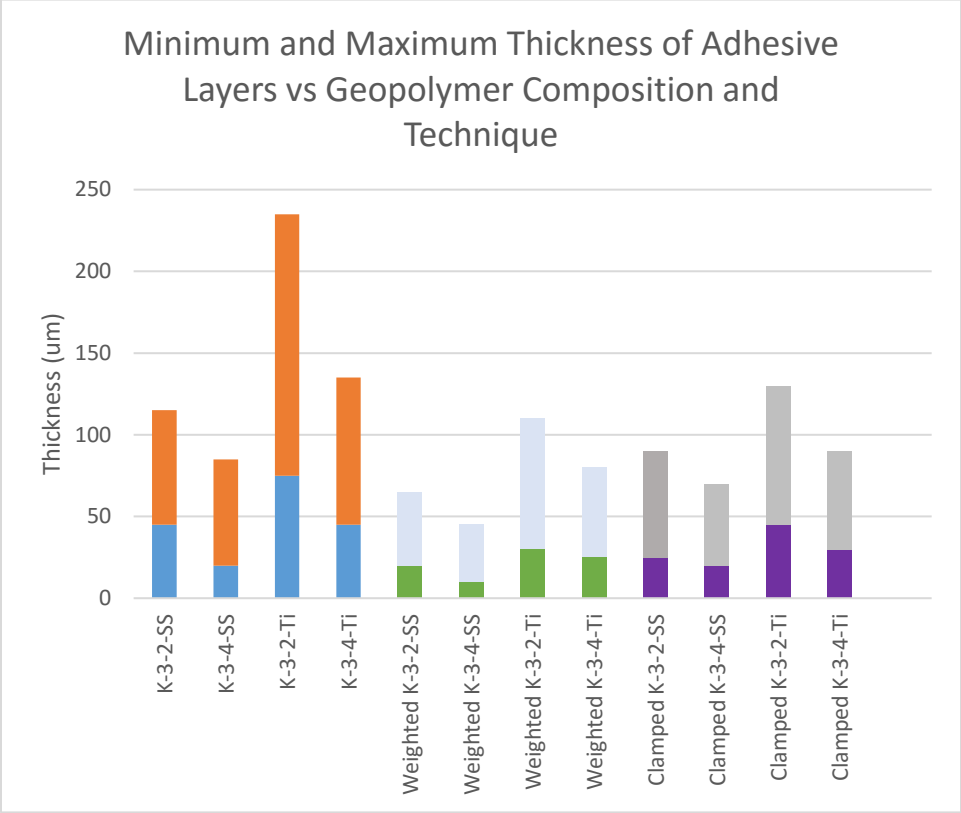

Figure 24: Plot of minimum and maximum adhesive gaps for various geopolymer compositions and fixturing methods

It can clearly be seen that the K-3-4 geopolymer produces the thinnest adhesive layer with the stainless steel substrate, followed by the K-3-2 geopolymer with the stainless steel substrate. Counterintuitively, the K-3-4 geopolymer with the titanium substrate actually in almost all cases produces a thicker adhesive layer than the K-3-2 geopolymer in conjunction with the stainless steel substrate. This may be attributed most likely to the higher surface roughness and interaction of the viscous gel with the substrate surface. It can be speculated here that during adhesion, a smoother contact surface allows the gel to

move more readily and therefore be more easily dispelled out the sides of the specimen being adhered. For all lap shear specimens analyzed, the weighted method was used while the clamped method was used for all tensile specimens.

4.3 Analysis of Cross Section

4.3.1 Electron Microscopy

The sectioned specimens were also used to examine the mechanical interlocking between the substrate and the adhesive. Using an electron microscope, the boundary between the substrate and adhesive was analyzed in depth to determine critical surface features.

A titanium substrate with K-3-2 geopolymer adhesive is shown in Figure 25. On the right side of the picture we can clearly see the smooth metallic substrate while the left side shows the typical amorphous characteristic commonly associated with geopolymers. The discolorations on the far right side of the substrate are identified as silicon carbide by Energy-Dispersive X-ray Spectroscopy (EDS), possibly residual from polishing. On the metallic substrate, several ‘divots’ can be seen in which the geopolymer has become mechanically attached to the substrate. In addition, there is no cracking, delamination, or separation between the substrate and the adhesive. Similar results are seen in Figure 26, which shows a K-3-2 geopolymer adhesive with a stainless steel substrate. It should be noted, however, that the substrate and geopolymer adhesive are no longer level on the

same plane in the photo. This is probably due to uneven polishing, which eroded the softer geopolymer layer away more quickly than the substrate layer.

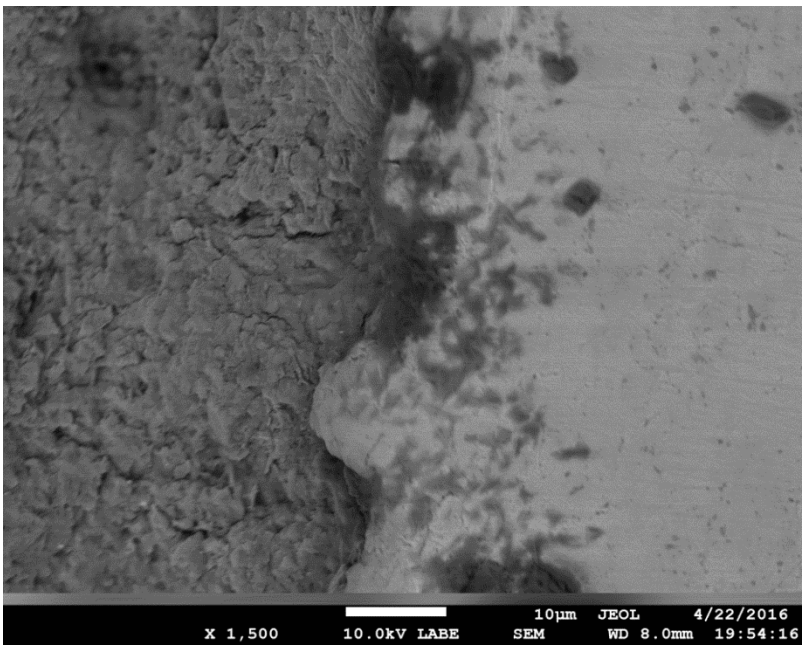

Figure 25:Titanium substrate (right) with geopolymer adhesive (left)

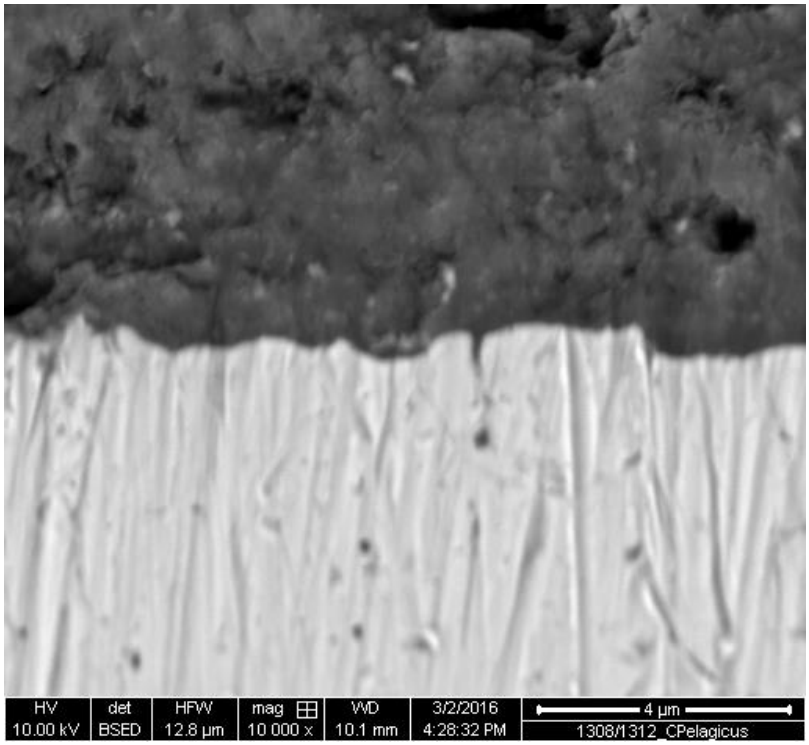

Figure 26: Stainless steel substrate (bottom) adhered with geopolymer adhesive (top)

Figure 27, shows a higher magnification of the interface between geopolymer adhesive (K-3-2) with titanium substrate with one of the deeper gaps seen in the substrate surface. It appears that the geopolymer gel has infiltrated this gap leading to an increased mechanical interaction. Micro cracking in the geopolymer near the substrate can also begin to be seen here, as mechanical stresses near the interface are increased. This micro cracking can be better seen in Figure 28.

Figure 27: Flaw on titanium substrate surface infiltrated by geopolymer gel

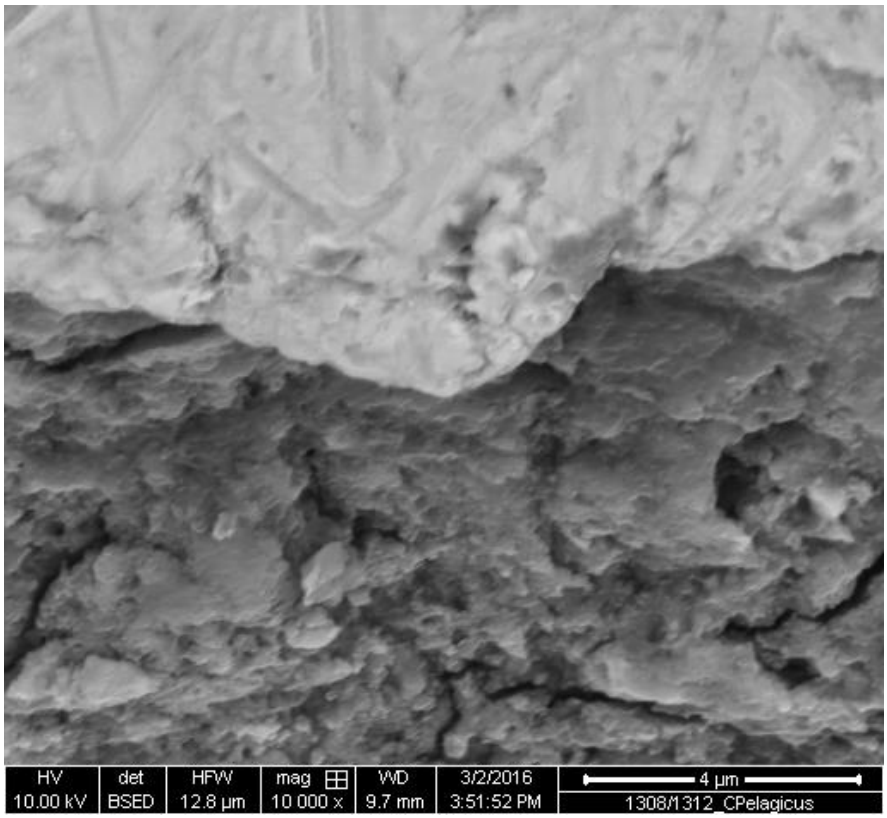

Figure 28: Microcracking in geopolymer (bottom) near titanium substrate surface

4.3.2 EDS Analysis

EDS was used in order to determine the chemical makeup of the materials on both sides of the interface and to determine if there was any chemical interaction between the geopolymer gel and the metallic substrates.

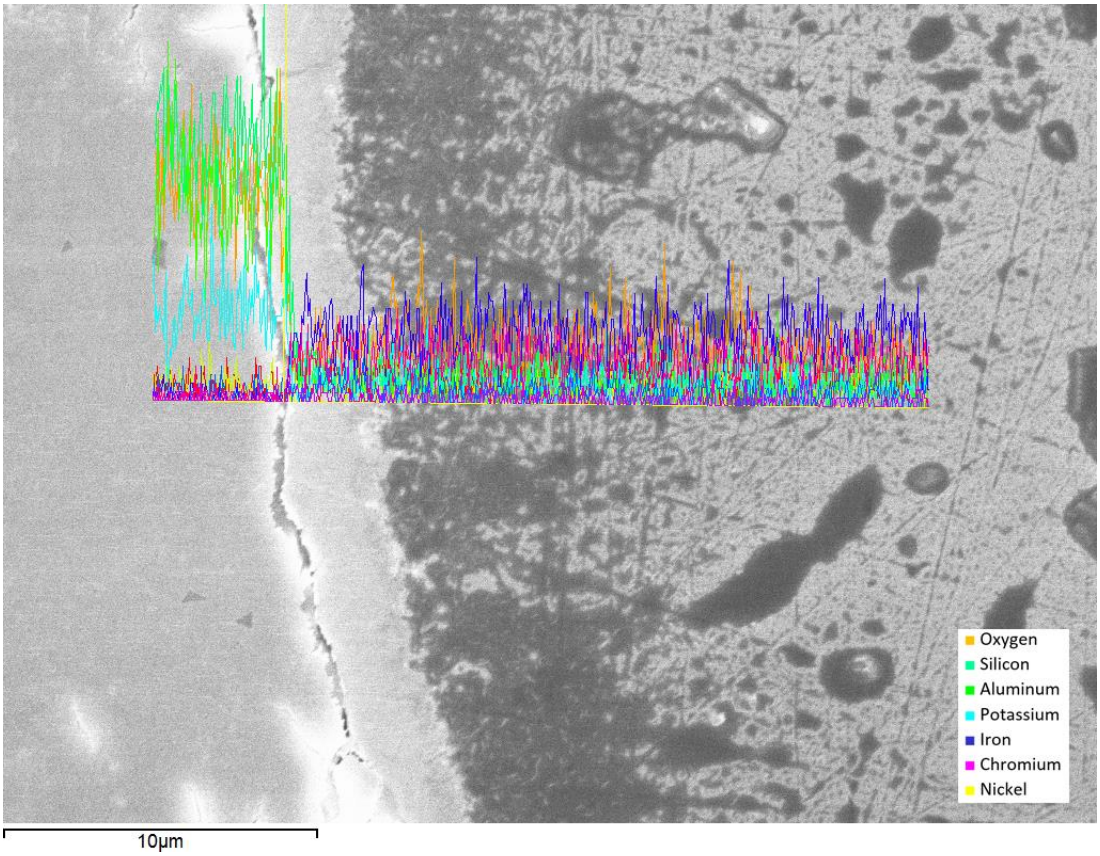

Figure 29: EDS analysis of boundary between geopolymer (left) and stainless steel substrate (right)

In Figure 29 the geopolymer/substrate boundary is clearly defined by an EDS line scan. At the interface the concentrations of aluminum, silicon, and potassium drastically decrease while the concentration of iron and chromium increase (for a stainless steel substrate). We see a similar result in Figure 30 with a titanium substrate, where the aluminum, silicon, and potassium content drops off rapidly at the interface while the titanium concentration increases.

One thing that is consistent between these results is the behavior of the oxygen concentration throughout the interface. In Figure 30 the oxygen line can be seen in

orange. Closer inspection reveals that while the oxygen content remains high in the geopolymer as expected, the concentration does not immediately drop off at or immediately after the interface (due to an oxide layer). Instead, the oxygen content tapers down over a distance of approximately 10um until it reaches a steady value in the material. This can also be seen in Figure 29, but is more difficult to observe due to the more complex alloy.

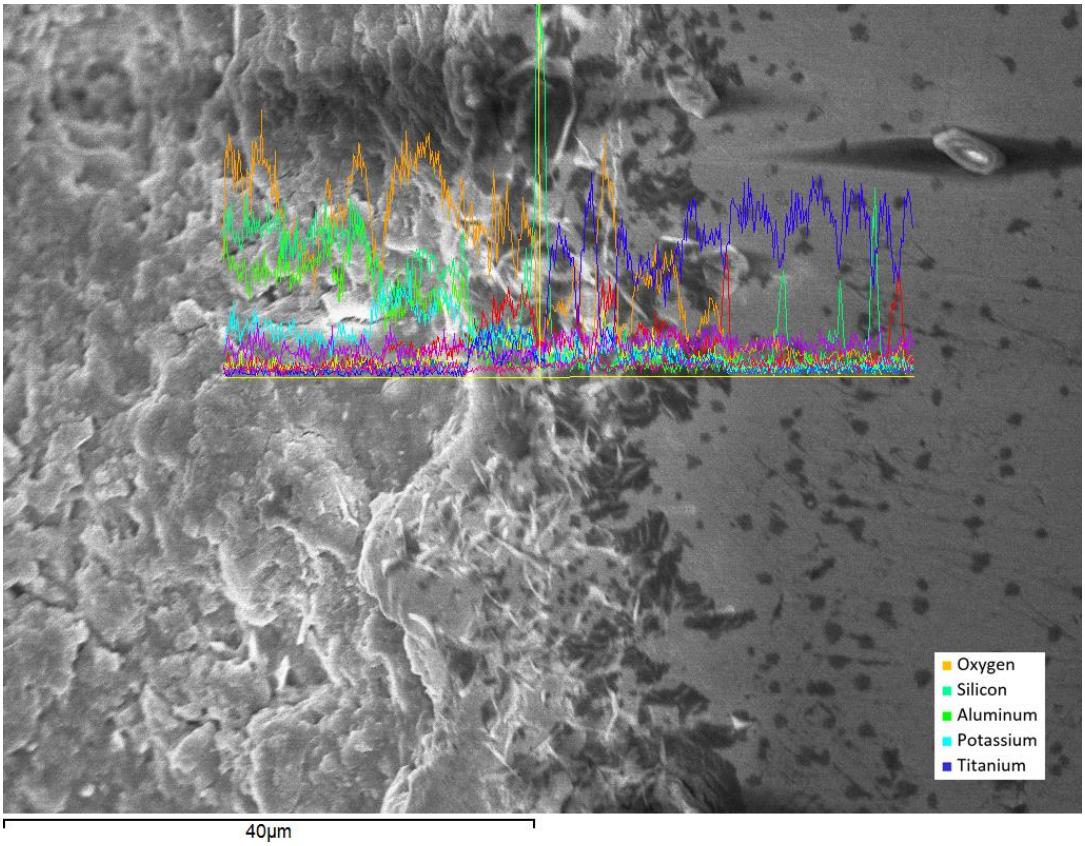

Figure 30: EDS analysis of boundary between geopolymer (left) and titanium substrate (right)

4.4 Shear Testing

4.4.1 Shear Strength Results

Shear testing was performed using a single lap shear test. The results of these experiments can be seen in Figure 31.

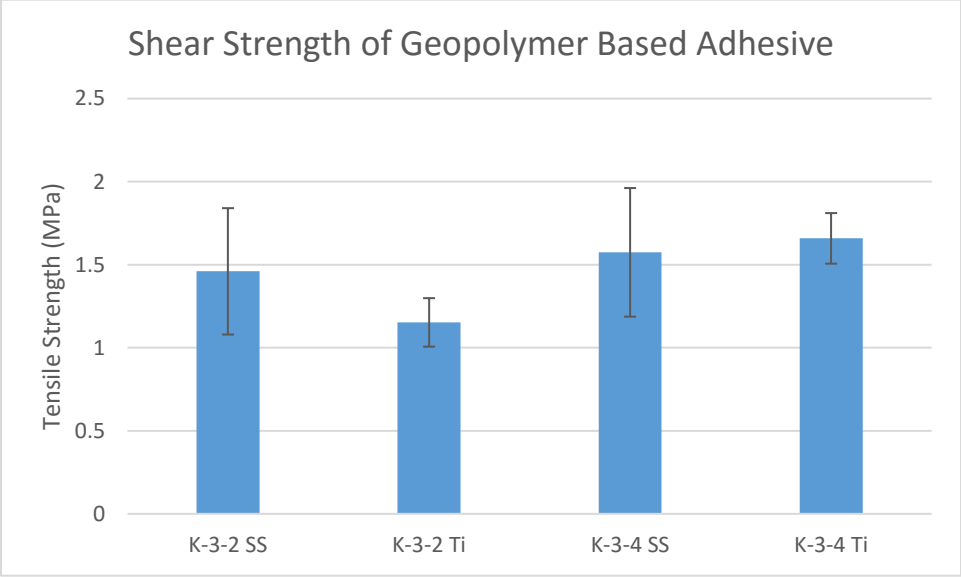

Figure 31: Lap shear test results for various substrates and geopolymer compositions

It can be seen that samples with stainless steel substrates exhibited higher shear strengths than those with titanium substrates, in addition to the thinner K-3-4 geopolymer based adhesive exhibiting slightly higher shear strength than the thicker K-3-2 geopolymer. This may be due to the thickness of the adhesive layer; the thinner layer allows for higher strength due to a higher proportion of the adhesive layer exhibiting oxygen bridging with the substrate surface.

4.4.2 Optical Microscopy Analysis

An analysis of the shear specimens was conducted using optical microscopy. Typical images of the failed substrate surfaces can be seen in Figure 32.

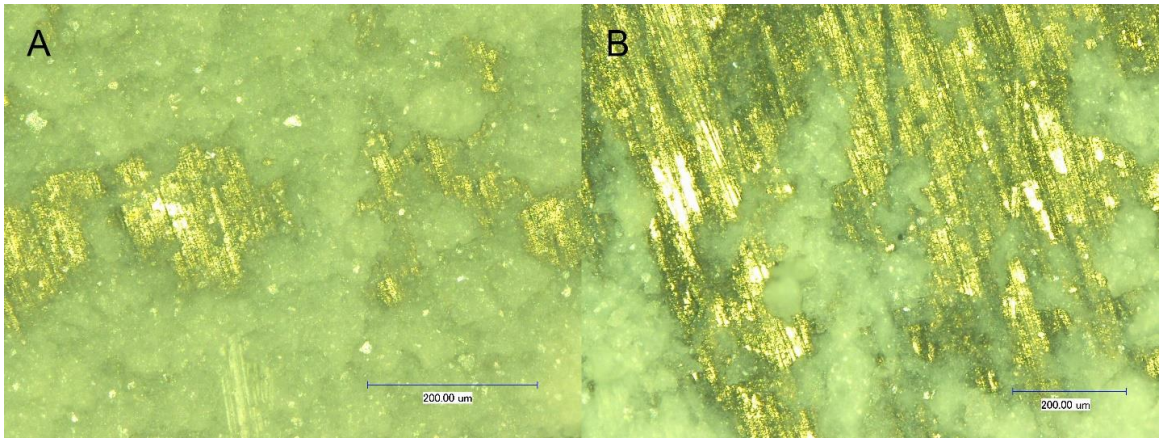

Figure 32: Surface of failed shear specimens for stainless steel substrate (A) and titanium substrate (B)

It can be seen that the crack propagation in shear is partially through the matrix. Therefore, the failure is not due to delamination. It appears that the failure mode is dictated by crack propagation in shear, which correlates well to other researched results as previously discussed.

4.5 Tensile Testing

4.5.1 Tensile Strength Results

Tensile strength was tested using a pure tension setup to derive the most accurate results. Initial results showed that the lower water content K-3-2 geopolymer seemed to give higher strength, so more tests were performed with that composition. 8 specimens were prepared for each substrate with the K-3-2 geopolymer gel, and 4 specimens were prepared for each substrate with the K-3-4 geopolymer gel. The specimens were adhered using a jig to align the specimens and clamped with approximately 20N of force during curing.

The loading for each specimen was set to be at the constant displacement rate of 0.05 in/s. Each specimen seemed to have a similar loading curve, an example of which can be seen in Figure 33. Each curve began with very low load while the fixture was preloading shown in segment A, followed by a short period of rapid loading as shown in segment B. After this initial rapid loading, another segment of slow loading occurs as shown in segment C. This is theorized to be due to the threads on the sample slowly coming into full contact with the threads on the test frame. Once the threads are in full contact, the load quickly increases until the specimen fails as shown in segment D of the diagram.

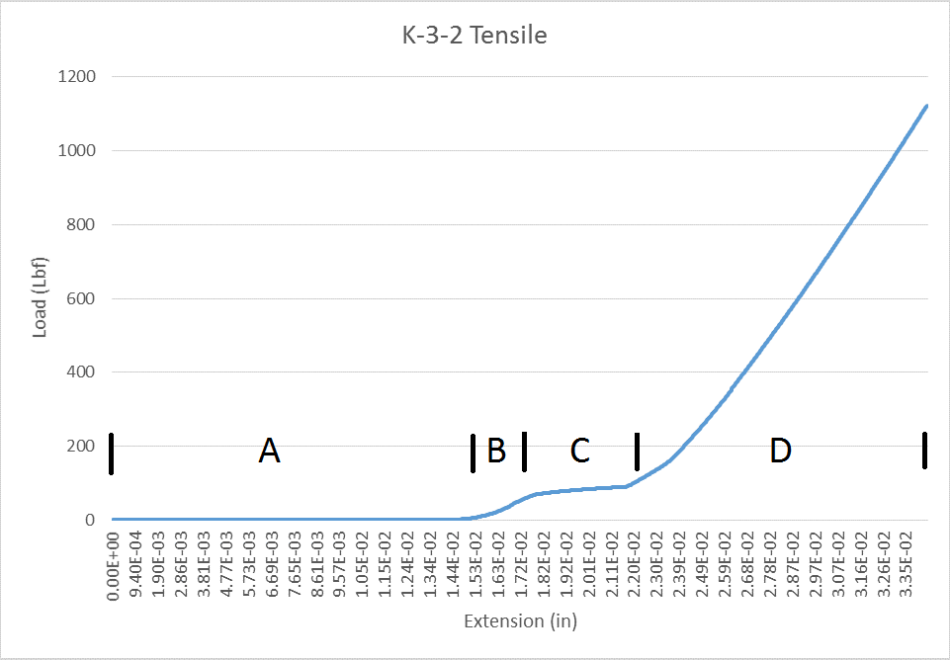

Figure 33: Typical loading curve for tensile testing

The tensile strengths of different samples can be seen in Figure 34. Stainless steel substrates bonded with K-3-2 geopolymer adhesive exhibited the highest tensile strength with an average (standard deviation) value of 5.9(3.24) MPa. This is followed by the Titanium substrates bonded with K-3-2 geopolymer adhesive at 4.4(2.64) MPa, then the Stainless Steel substrate bonded with K-3-4 adhesive at 1.95(2.50) MPa and finally, the Titanium substrate bonded with K-3-4 adhesive at 1.25(1.61) MPa. Due to the high standard deviation of the results, it is suggested that more tests be performed and a statistical Weibull analysis be conducted in order to provide more accurate statistical data.

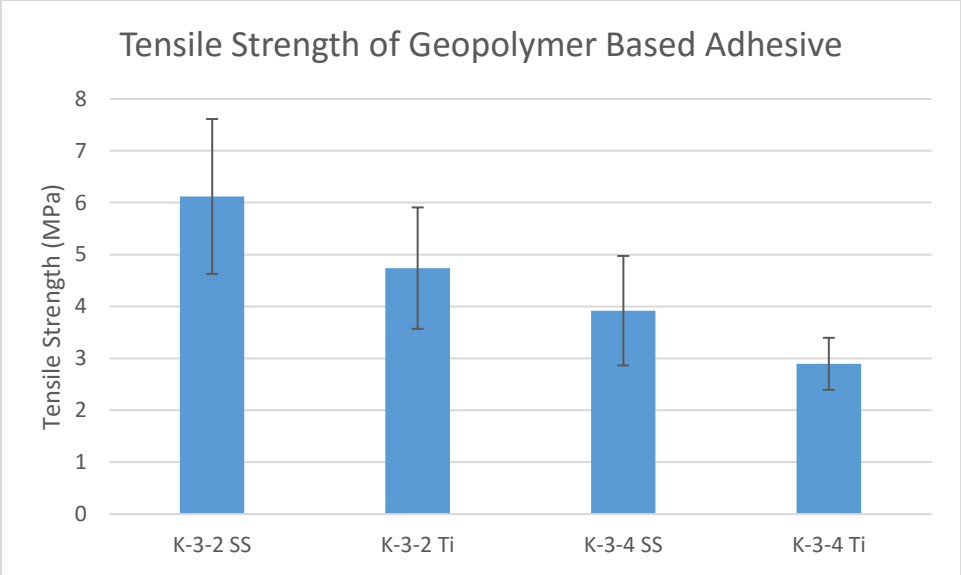

Figure 34: Tensile strength results of various substrates and geopolymer compositions

The difference in the modes of failure between the high strength and low strength specimens should be noted. The specimens failed in one of several modes observed by visual inspection of the fracture surfaces and depicted in Figure 35: Pure shear break as seen in segment A, mixed break as seen in segment B, or delaminated break as seen in segment C. The specimens that failed in the pure shear mode exhibited the highest strength, followed by the specimens that failed in mixed modes and finally delaminating modes.

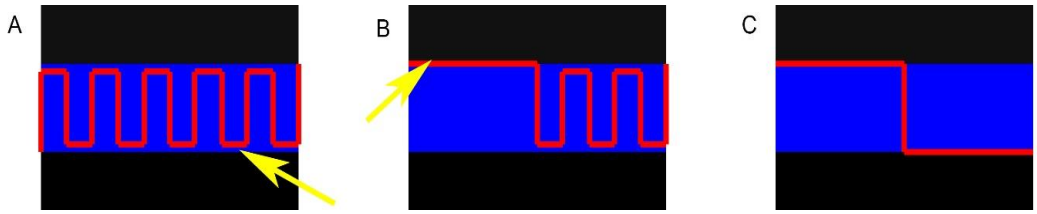

Figure 35: Tensile failure modes - A: Full shear, B: Mixed break, C: Delaminated break

It should be noted that the pure shear failure mode fractures do not go all the way to the substrate, but rather leave an extremely thin layer of geopolymer adhesive between the substrate and the fracture surface. This supports the theory of oxygen bridging being present between the metallic oxide layer and the silicon in the geopolymer gel, as it would take more energy for the fracture to propagate through the chemically bonded layer than it does for it to propagate through the geopolymer matrix. The path of the fracture requires the geopolymer to shear multiple times and thus expend much energy to propagate the fracture through the matrix, resulting in a very high tensile strength.

In the mixed modal and delaminated failures, the geopolymer separated from the metallic substrate in either partially or entirely. It is unclear what causes this delamination but it is suspected to be due to poor sample preparation by making the matrix too thick during curing, or failure to properly remove all oils from the specimen surface prior to applying the geopolymer adhesive. In these specimens, the fracture does not have to expend nearly as much energy to propagate through the geopolymer matrix, and thus leads to a lower tensile strength.

In addition to the failure modes, it appears that some of the specimens that failed at a drastically lower load did not seem to be fixed in the jig properly while being cured, leading to uneven adhesion. If the adhesive coating was thicker on one side of the specimen than the other, it could induce a bending moment on the specimen and result in a different mode of failure, leading to a premature break (sometimes even while securing them to the tensile frame). These results were removed from the data shown above, but caution should be taken to avoid this failure mode during testing.

4.5.2 Optical Microscopy Analysis

Optical microscopy after tensile failure on multiple specimens confirms the presence of the aforementioned three failure modes. Figure 36 depicts pure shear failure and mixed mode failure on a titanium surface in segments A and B, and pure shear failure and mixed mode failure on a stainless steel surface in segments C and D, respectively.

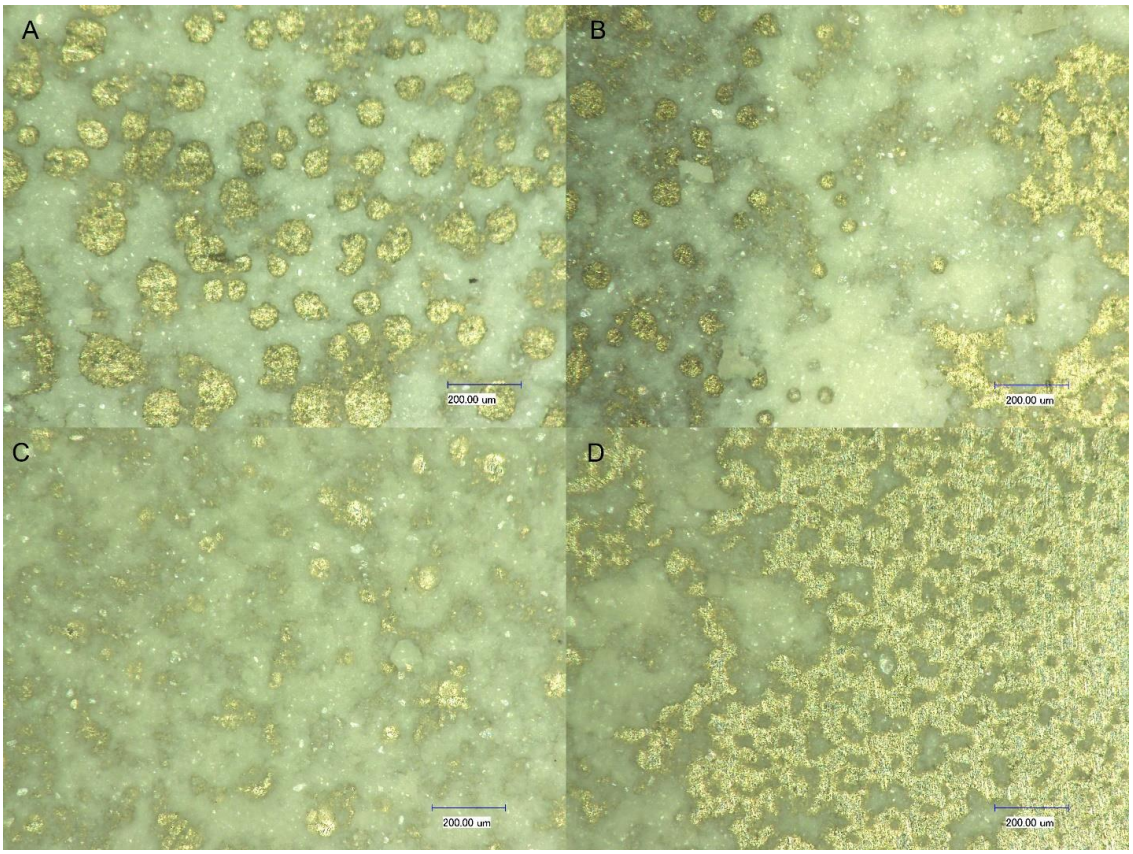

Figure 36: Optical analysis of failed tensile specimens. A and C represent high strength failure while B and D represent low strength failure

While only one surface of the failed tensile specimen is shown in segments A and C, the other half of the tensile specimen looks nearly identical with a similar distribution of similar sized of geopolymer “patches” or islands on the surfaces . This confirms the shear failure mode allows fracture propagation via shearing through the geopolymer matrix. In addition, while it appears that substrate is exposed through the ‘holes’ in the optical microscopy photos, further inspection via SEM and EDS reveals it is actually still covered in a nanometers thick coating of geopolymer adhesive. In the mixed modal

failures (segments C and D) large patches of geopolymer and metallic substrate can be seen, indicating a minimal amount crack propagation due to shearing through the geopolymer matrix.

Each of the ‘pores’ ranges in diameter from approximately 40 um to 150 um for the titanium substrate, and 20 um to 100 um for the stainless steel substrate. Smaller pores allow for higher pore density; since the failure mode for these specimens involves shear failure along the pore ‘walls’, this may indicate why the specimens with a stainless steel substrate exhibited higher tensile strength than the specimens with a titanium substrate.

4.5.3 Electron Microscope Analysis

Electron microscopy confirms the results discovered by optical microscopy and tensile testing. A closer inspection of several of the pores can be seen in Figure 37, where segments A and B show a close up of two pores while segments C and D show a detail of one of the side walls of the pore.

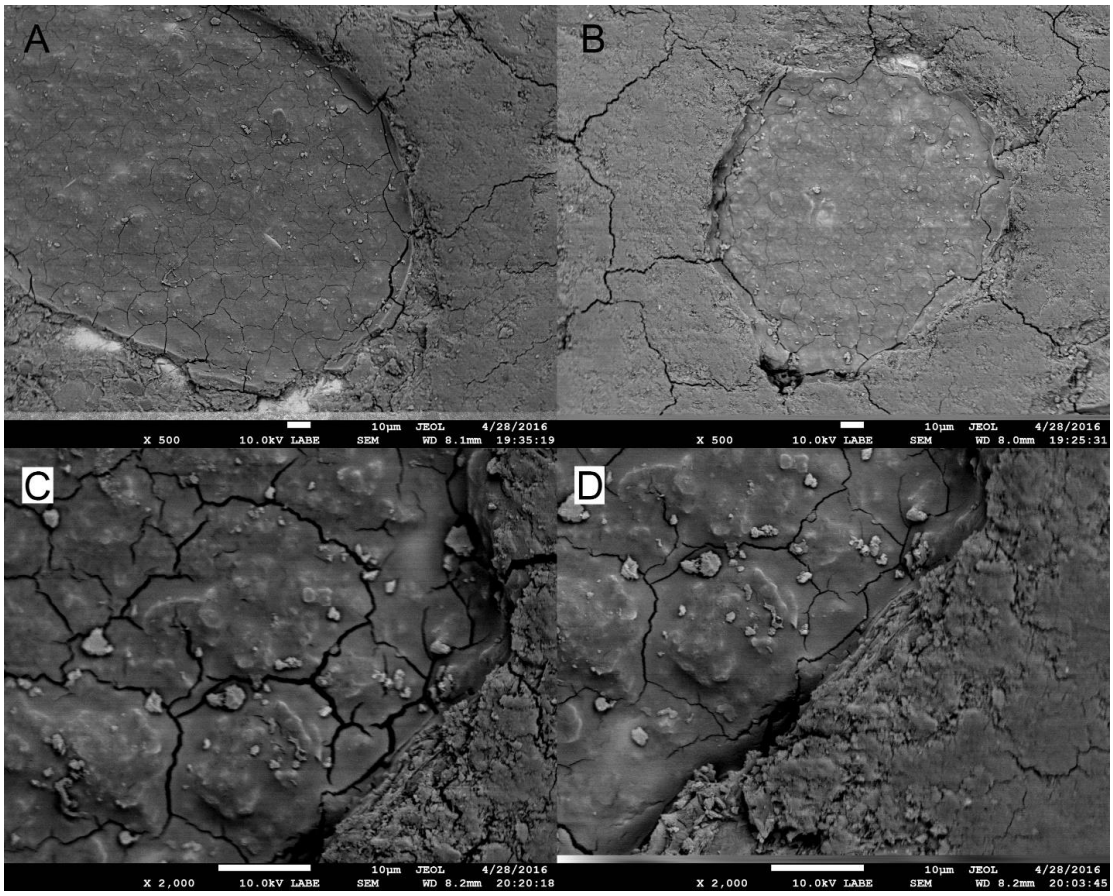

Figure 37: SEM analysis of pores on surface of failed tensile speciemen

As previously stated, the substrate is not exposed through the pore but rather coated by a nanometers thick geopolymer coating. Closer inspection of the surface surrounding the pores in segments A and B indicates the pores may be created by the merging of microcracks in the surface into a closed path, providing a reduced thickness area that is more easily sheared through.

4.5.4 EDS Analysis

In order to better understand the chemical interaction between the substrates and the geopolymer adhesive under stress, and EDS analysis was conducted on the surfaces of the fractured tensile specimens. Figure 38 depicts EDS elemental analysis along a scanning line crossing the pore.

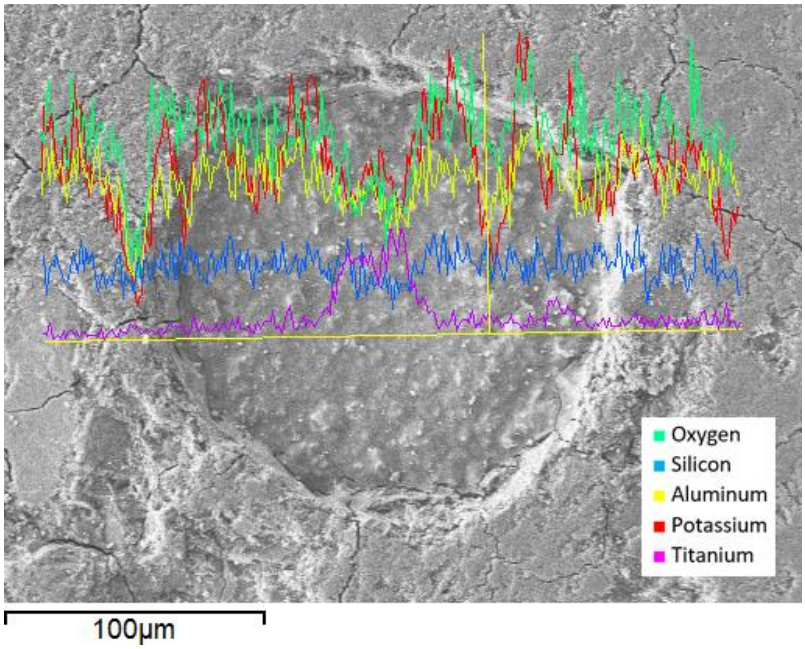

Figure 38: EDS analysis of pore found on failed tensile surface

The line scan shows a higher concentration of titanium (purple) throughout the center of the pore, with a reduction in aluminum (orange) and potassium (red) where the titanium concentration is higher. However the silicon (blue) does not exhibit as much of a

reduction in concentration where the titanium concentration is elevated. These results support the theory that the geopolymer layer at the bottom of the pore is thin on the order of nanometers in order to detect significant concentrations of titanium. In addition, the coexistence of oxygen, silicon, and titanium at the center of the pore may indicate the presence of Si-O-Ti bonding.

While the line scans are useful, a qualitative mapping of the surface of a pore produced much more in depth results that can be seen in Figure 39. The first segment shows an overall view of the mapping area, while the 5 other segments show the individual relative concentrations of aluminum, potassium, oxygen, silicon, and titanium across the pore.

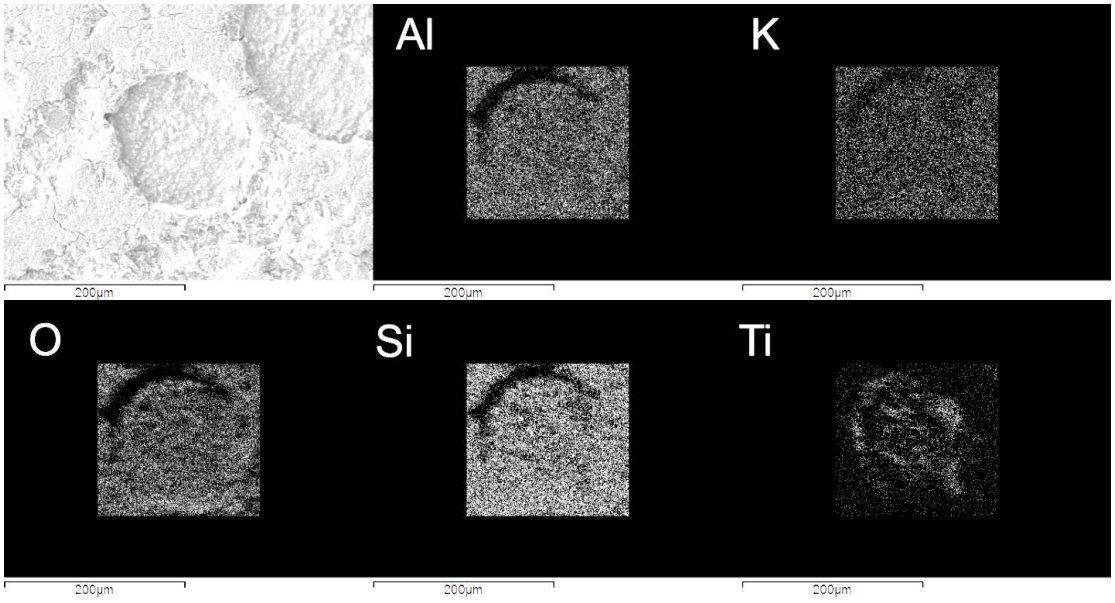

Figure 39: EDS mapping of pore found on failed tensile surface

The higher titanium concentration on the top left hand side of the mapping, along the ridge of the pore may be indicative of the location of the failure propagation. When the crack first begins to propagate, it may penetrate almost to the substrate interface. However, due to the oxygen bridging occurring at that interface, the crack then propagates upward through the geopolymer matrix as it requires less energy. This failure mode can be seen in Figure 40, where the arrow depicts the area where more energy is required for crack propagation.

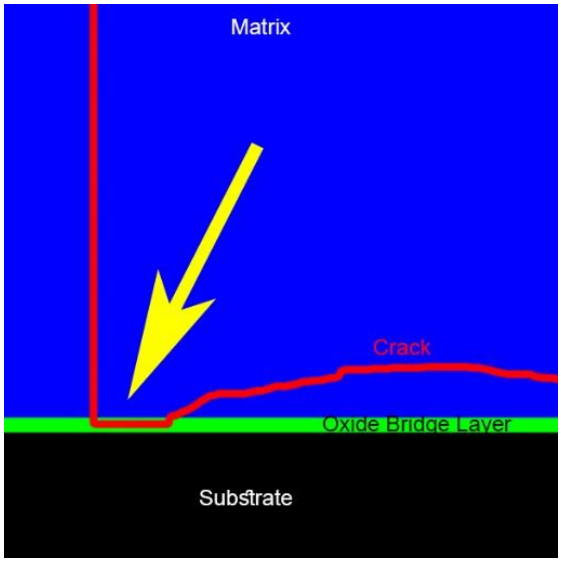

Figure 40: Graphical explanation of shear crack propagation through geopolymer matrix

It can be clearly seen that the higher concentrations of titanium correlate to the lower concentrations of the other elements in Figure 39, indicating a thin area in the coating on the bottom of the pore. However, a careful analysis overlaying the silicon and titanium

mappings shows some interaction between the two. This overlaid mapping can be seen in Figure 41.

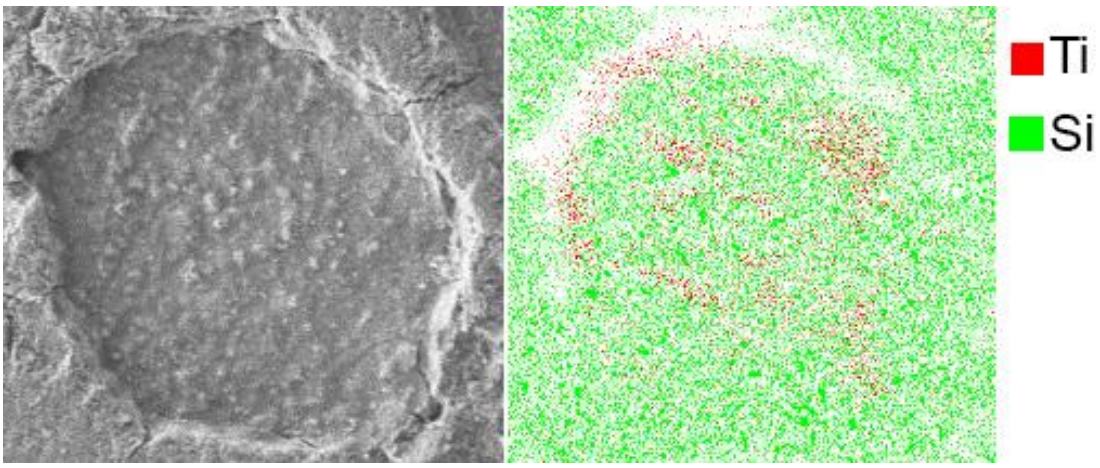

Figure 41: EDS comparison of concentrations of Si and Ti in pore found on failed tensile surface

4.6 Heat Treatment

Samples were also subjected to elevated temperatures to test their durability when exposed to high temperature environments. No debonding was observed in more stainless steel or titanium coupons that were glued with K-3-2, K-3-4, K-4-2, or Na-3-2 geopolymer, after heat treatment for one hour up to 100, 200, 300, 500, 600, 700 and 800 ^{o}C. Specimens analyzed via SEM were heated to 800 ^{o}C, while tensile and shear specimens were heated to 500 ^{o}C for 1 hour, and the cooled down to the room temperature before tensile testing.

4.6.1 Electron Microscopy

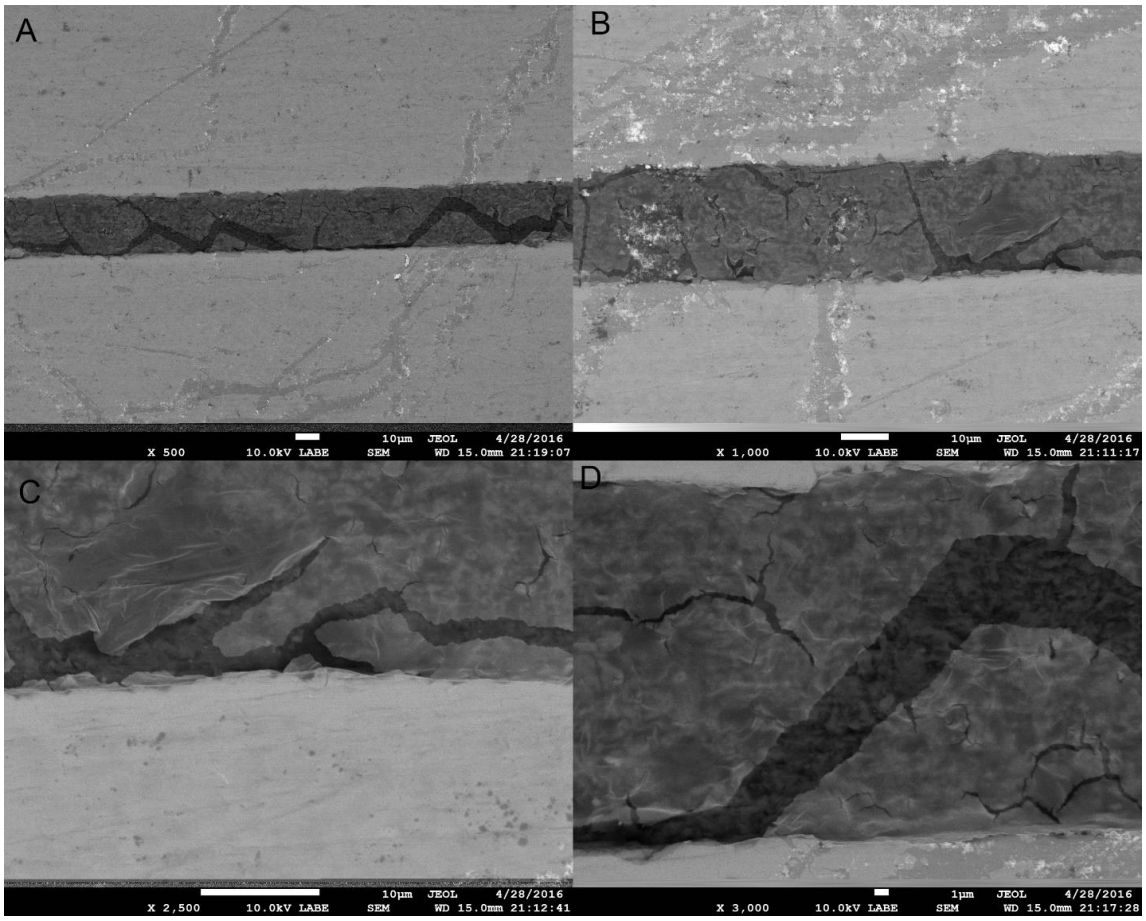

Figure 42: SEM analysis of heat treated specimens

Electron microscopy revealed an interesting cracking pattern in the heat treated specimens. Upon heating, the specimens showed a zig-zag shaped pattern that propagated through the geopolymer matrix. This zig zag is best seen in segments A and D of Figure 42. In addition, in other areas cracks propagated from one substrate surface to the other, as seen in segments B and C of Figure 42. These cracks and zig-zag patterns

can easily be explained by the stresses induced by the difference in thermal expansion between the geopolymer adhesive and the metallic substrate. Since the metallic substrate has a much higher thermal expansion coefficient than the ceramic based geopolymer, upon heating the metallic substrate stretches and cracks the geopolymer through the matrix. Theoretically, however, it does not cause complete debonding due to the chemical bonding between the matrix and substrate.

4.6.2 Tensile Results

The room temperature tensile strengths of the specimens after heat treatments at 500 ºC for 1 hour are provided in in Figure 43. Due to time and budget constraints, heat treated shear specimens were not tested in this work.

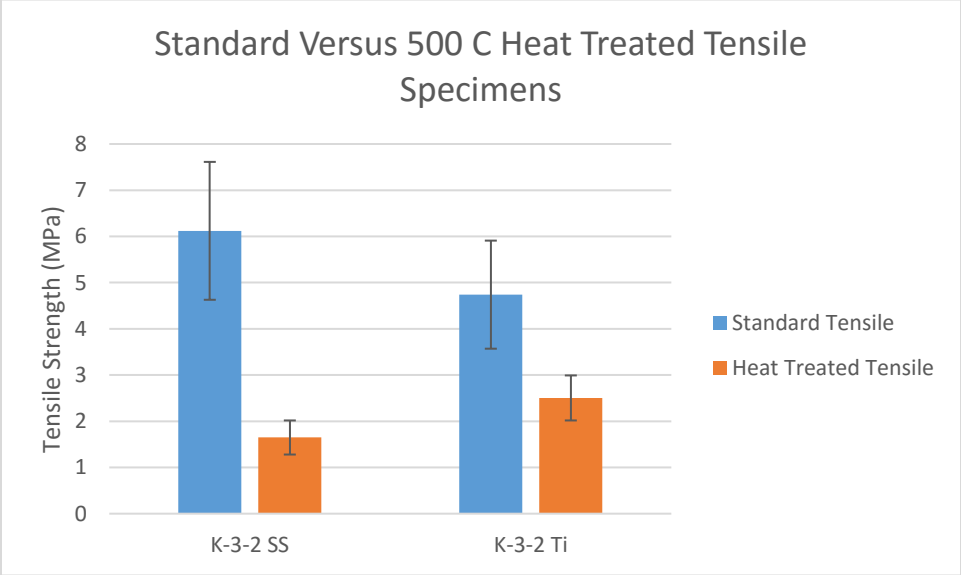

Figure 43: Tensile strength of heat treated specimens

The heat treated specimens exhibited approximately 25 to 50 % of the tensile strength of the non-heat treated specimens.

4.6.2.1 OPTICAL MICROSCOPY ANALYSIS

An optical analysis of the failed surfaces of the heat treated tensile specimens, seen in Figure 44, reveals patterned pores similar to those found in the standard tensile specimens. However there are several differences, notably the shape of the pores. While the pores found in the standard failed tensile specimens are round or ellipsoid as seen in Figure 36, the pores found in the failed heat treated tensile specimens are polygonal. This could be due to the shear cracks propagating through the existing thermal expansion cracks, leading to ‘sharp’ corners where thermal expansion cracks intersect.

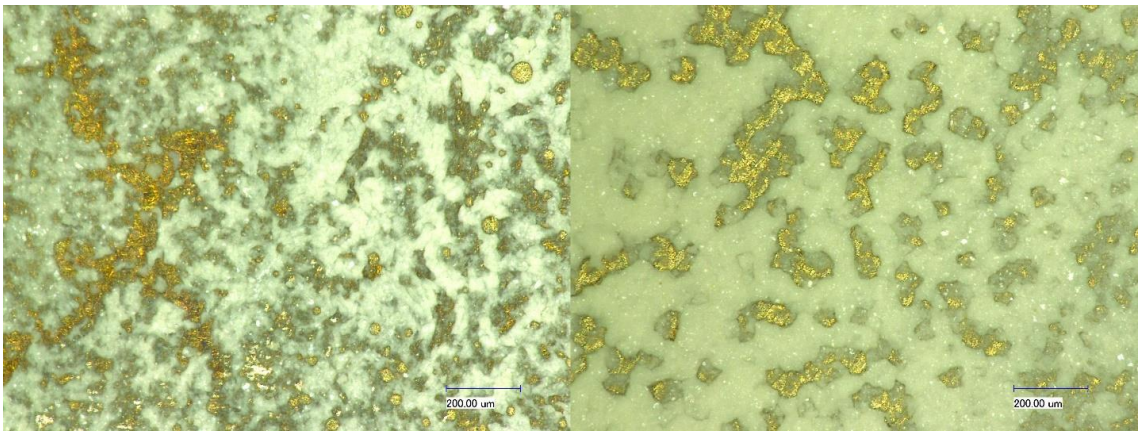

Figure 44: Optical micrographs of heat treated specimens. A: Stainless steel substrate, B: Titanium substrate

4.7 Polished Specimens

In order to evaluate the degree of chemical interaction versus mechanical interaction in the geopolymer adhesive with the substrate, several specimens were polished to a mirror finish and testing in tension. Mirror finishing provided very smooth surfaces of the substrates and thus less mechanical interlocking between adhesive geopolymer layer and the substrate. Figure 45 shows the results for both polished stainless steel and titanium substrates adhered with K-3-2 Geopolymer adhesive. For comparison, the results obtained using unpolished samples from Figure 34 are also presented in this figure.

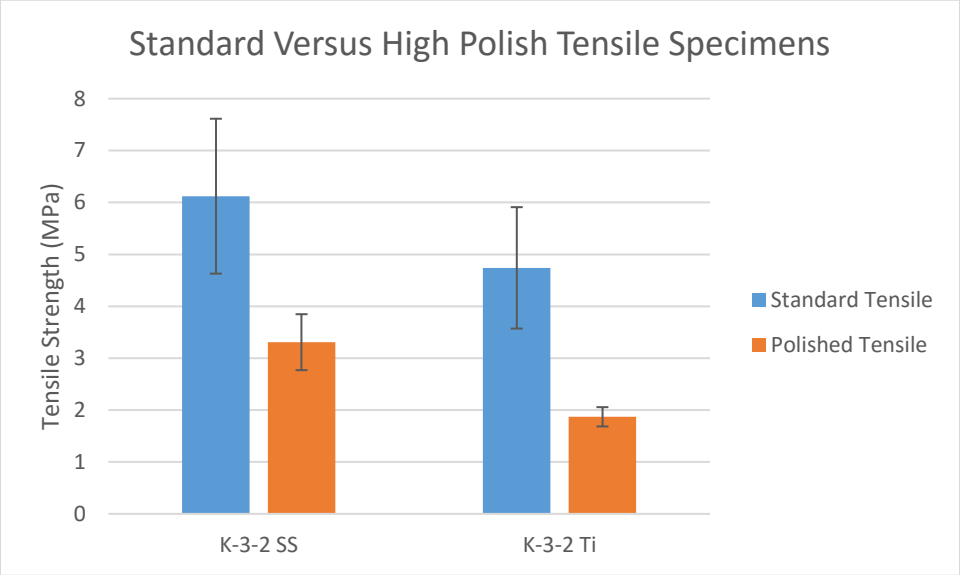

Figure 45: Tensile strength of specimens with mirror polished substrates

The average tensile strength of both the titanium and the stainless steel substrates are approximately 50% of the average tensile strength from the tests performed earlier using only ground metallic substrate surfaces. This can be explained by higher smaller surface

roughness of the mirror polished metallic surface as surface roughness not only provided better mechanical interlocking but increased surface area for oxygen bonding to possibly take place.

In addition, some of the polished specimens were exposed to an elevated temperature of 500 ^{o}C for 24 hours before cooled down to the room temperature and tensile testing to determine the effect of surface polishing and heat treatments on the tensile strength of the adhesive. The specimens were then tensile tested, with results shown in Figure 46.

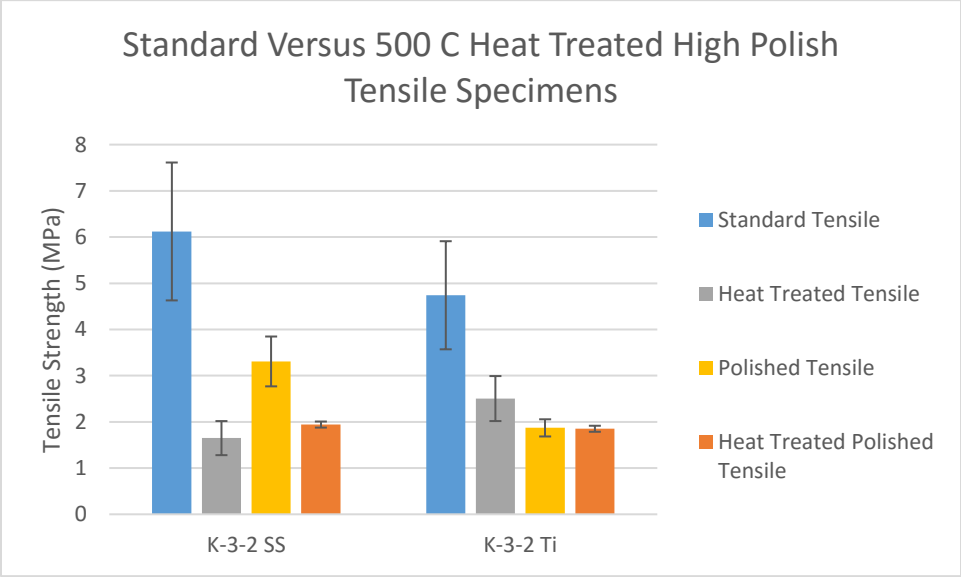

Figure 46: Tensile strength of specimens with mirror polished substrates with heat treatment

It can be seen that the results correspond to the difference in standard tensile specimens and standard heat treated specimens, with a reduction in strength of approximately 60 percent.

5 CONCLUSION

Results of this study show that geopolymer can be used as high temperature adhesive for titanium and stainless steel, and possibly other metals and alloys. A comparison of alternative commercially available adhesives with geopolymer based adhesive can be seen in Table 2. When the shear strengths were compared to other commercially available polymeric adhesives, geopolymer adhesives studied here show lower or comparable shear strength, however unlike polymeric adhesives they can be used to substantially higher temperatures, possibly exceeding even 800 °C. On the other hand, when compared to other commercial ceramic adhesives that can be used at higher temperatures, they show much higher shear strength.

Table 2: Comparison of geopolymer based adhesive to other commercially available adhesives for metallic substrates [44-47]

	Max Shear Range (MPa)	*Max Operating Temperature (°C)*	*Fireproof*
Geopolymer	1-6	750	Yes
Cyanoacrylate	5-15	82	No
RTV Silicone	0.8-1.5	180	No
Ceramic	0.1-0.7	1650	Yes
Instant Epoxy	8-20	50	No
Silane Polymer	1-4	50	No
Metal Epoxy	8-24	140	No

Comparison of the results of the various tests performed in this work show evidence not only of mechanical interaction (interlocking) but also of a chemical interaction between the metallic substrate and geopolymer adhesive layer. The latter is most likely the reason for the good mechanical properties of the geopolymer adhesives when compared to other ceramic adhesives.

First, a comparison between the standard tensile test specimens with a rough surface and the polished tensile test specimens with a mirror surface shows that the adhesion is not purely mechanical, as the polished layer possessed little to no surface roughness for the geopolymer adhesive to physically interlock with. Thus a chemical bond must exist in order to explain the results obtained by the polished tensile test specimens. While the polished specimens did possess higher than expected tensile strength, they still were only capable of supporting approximately 50 percent of the load of the standard tensile specimens with a rough surface finish. These results can be explained by two theories: the higher loads in the standard samples are due to a combination of chemical and mechanical interactions, or the higher loads in the standard specimens are due to an increased amount of chemical bonding due to the increased surface area on the uneven surface of the standard specimens. Most likely the true reason for the higher strength in the standard tensile samples is a combination of these two. Further research is required to determine the degree of mechanical versus chemical interaction is responsible for the tensile strength.

Specimens subjected to heat treatment exhibited higher than expected tensile strength, but still significantly lower strength than non-heat treated specimens at approximately 40 percent of the non-heat treated strength. As previously stated, this is speculated to be due to the higher thermal expansion coefficient in the metallic substrate. During heating, the expanding metal imposes a biaxial tension on the geopolymer adhesive, causing it to crack throughout the matrix perpendicular to the substrate surface. These cracks, while weakening the overall structure, do not seem to run parallel to the substrate surface at any location and thus do not lead to delamination. During tensile testing after heat treatment, the cracks formed by thermal expansion provide a starting point for the shear crack propagation failure mode seen in other standard tensile specimens; as the load increases the cracks join and form enclosed areas, which are then capable of easily shearing through the matrix. At this point the specimen fails. It should be noted that the heat treated polished tensile specimens failed at almost the same load that their non-heat treated polished counterparts failed at. The reason for this is still not clear at this point, but since in booths samples with polished and ground surfaces, thermal treatment leads to the formation of the zig-zag microcracks in the geopolymer adhesive due to thermal expansion mismatch. Although more work is needed to further understand this phenomenon, we can hypothesize at this point that initial zig-zag microcracks due to thermal expansion preferentially originate at deep dimples and surface crevices filed with geopolymer – such as those shown in Figure 25, leading to the larger number of zig-zag crack in heat treated samples with ground surfaces, when compared to those with mirror polished surfaces.

5.1 Future Work

While the aforementioned results are indeed conclusive, further testing could solidify the theories and mechanisms proposed in this work. Several suggestions that would improve this study have been included as suggestions for future research work on this topic.

5.1.1 Weibull Statistics and Sample Size

Due to the ceramic nature of the geopolymer adhesive, the failure loads of both the shear and tensile tests are relatively inconsistent. By utilizing Weibull statistics in future research, the tensile and shear strengths can be measured much more quantitatively than with simple mean and standard deviation measures. In addition, a larger sample size would provide much more consistent data than the small sample size used in this work.

5.2 XPS

In this work an oxygen bridging between the geopolymer adhesive and substrate was theorized due to the analysis of physical failure behavior and the chemical spectrum of the surface after failure. However, XPS could provide a much better indication of the chemical bonding at the interfaces. Several researchers have done work with Si-O-Ti bonding and analyzed their results using XPS and established techniques to determine its presence [61, 62]. An XPS analysis of the substrate-adhesive interface layers could determine the presence and/or degree of oxygen bridging occurring.

5.2.1 Nano FTIR

While FTIR was conducted in this study (not shown here) in an effort to observe a characterizing shift for a Si-O-Ti bond, no useful results were obtained due to the relatively large sample area required by the standard FTIR instrumentation (3mm diameter). Another method, referred to as Nano IR, operates on the same principles as FTIR but does so on a microscopic level, allowing the user to precisely select the site of interest down to the nanometer level [63]. Using Nano FTIR with ATR, comparison of the pores found in the failed specimen's geopolymer layer to standard geopolymer and titanium oxide could show a characteristic shift of resonant light indicating an oxide bridge (research has shown that FTIR is capable of detecting a Si-O-Ti bond [64]).

5.2.2 Alternative Substrates

Titanium and 316 Stainless Steel alloy were tested in this work, but any metallic substrate that readily forms an oxide layer theoretically should perform well with geopolymer based adhesive. Other metallic substrates that would be useful to test include aluminum, Inconel, and ferrous steel.

5.2.3 Alternative Surface Preparation

This work has shown higher surface roughness of the substrate and coating is important to increasing the tensile strength of the specimen. This was theorized to be either due to

mechanical interaction, or due to additional surface area being created causing additional oxygen bridging to occur. Future works could seek to isolate this variable by carefully controlling surface area and roughness and determining the effectiveness of creating specimens whose physical properties are dominated by mechanical interaction (high roughness, low surface area) and chemical interaction (low roughness, high surface area).

5.2.4 Alternative Geopolymer Gels and Curing Conditions

The adhesive used on all specimens created in this work was synthesized from metakaolin based geopolymer gel. Another type of geopolymer gel is synthesized using industrial waste, namely fly ash. These fly ash based geopolymers can possess higher base amounts of silicon, and have shown promise for being a more ecologically friendly choice than metakaolin based geopolymers in recent research [36, 65]. Future research could determine if the silicon content in fly ash based geopolymers increases the degree of oxygen bridging a significant amount and therefore the shear and tensile strengths.

In addition, only two geopolymer ratios were tested in this work. These ratios were selected due to their midrange performance and ease of synthesis determined by previous research experience [12, 23]. Many other metakaolin compositions are capable of being synthesized with higher silicon, alkali, or water content. In theory, higher silicon content will lead to higher strength due to oxygen bridging while higher water

content will lead to a thinner adhesive layer. Future work may result in higher tensile and shear strengths due to optimization of these chemical parameters.

REFERENCES

1. V.D., G., *Gruntosilikaty*, G. Kiev, Editor. 1959: USSR.

2. Davidovits, J., *Geopolymer chemistry & application. Institute Géopolymèr-France, 2008.* ISBN: 9782951482012.

3. Bell, J.L., P.E. Driemeyer, and W.M. Kriven, *Formation of Ceramics from Metakaolin-Based Geopolymers. Part II: K-Based Geopolymer.* Journal of the American Ceramic Society, 2009. **92**(3): p. 607-615.

4. Davidovits, J., *Geopolymers and Geopolymeric Materials.* Journal of Thermal Analysis, 1989. **35**(2): p. 429-441.

5. Davidovits, J. *Environmentally driven geopolymer cement applications*. in *Proceedings of 2002 Geopolymer Conference. Melbourne. Australia*. 2002.

6. Duxson, P., et al., *The role of inorganic polymer technology in the development of 'green concrete'.* Cement and Concrete Research, 2007. **37**(12): p. 1590-1597.

7. Duxson, P., et al., *Geopolymer technology: the current state of the art.* Journal of Materials Science, 2007. **42**(9): p. 2917-2933.

8. Provis, J.L. and J.S.J. Van Deventer, *Geopolymers: structures, processing, properties and industrial applications*. 2009: Elsevier.

9. Hussain, M., et al., *Investigation of thermal and fire performance of novel hybrid geopolymer composites.* Journal of Materials Science, 2004. **39**(14): p. 4721-4726.

10. Cheng, T.W. and J.P. Chiu, *Fire-resistant geopolymer produced by granulated blast furnace slag.* Minerals Engineering, 2003. **16**(3): p. 205-210.

11. Van Jaarsveld, J.G.S., J.S.J. Van Deventer, and A. Schwartzman, *The potential use of geopolymeric materials to immobilise toxic metals: Part II. Material and leaching characteristics.* Minerals Engineering, 1999. **12**(1): p. 75-91.

12. Lizcano, M., et al., *Effects of Water Content and Chemical Composition on Structural Properties of Alkaline Activated Metakaolin-Based Geopolymers.* Journal of the American Ceramic Society, 2012. **95**(7): p. 2169-2177.

13. Rowles, M. and B. O'Connor, *Chemical optimisation of the compressive strength of aluminosilicate geopolymers synthesised by sodium silicate activation of metakaolinite.* Journal of Materials Chemistry, 2003. **13**(5): p. 1161-1165.

14. Buchwald, A., H. Hilbig, and C. Kaps, *Alkali-activated metakaolin-slag blends - performance and structure in dependence of their composition.* Journal of Materials Science, 2007. **42**(9): p. 3024-3032.

15. Fletcher, R.A., et al., *The composition range of aluminosilicate geopolymers.* Journal of the European Ceramic Society, 2005. **25**(9): p. 1471-1477.

16. Xu, H. and J.S.J. Van Deventer, *The geopolymerisation of alumino-silicate minerals.* International Journal of Mineral Processing, 2000. **59**(3): p. 247-266.

17. Phair, J.W. and J.S.J. Van Deventer, *Effect of the silicate activator pH on the microstructural characteristics of waste-based geopolymers.* International Journal of Mineral Processing, 2002. **66**(1-4): p. 121-143.

18. Fernandez-Jimenez, A., et al., *The role played by the reactive alumina content in the alkaline activation of fly ashes.* Microporous and Mesoporous Materials, 2006. **91**(1-3): p. 111-119.

19. Weng, L.Q., et al., *Effects of aluminates on the formation of geopolymers.* Materials Science and Engineering B-Solid State Materials for Advanced Technology, 2005. **117**(2): p. 163-168.

20. Duxson, P., et al., *Effect of alkali cations on aluminum incorporation in geopolymeric gels.* Industrial & Engineering Chemistry Research, 2005. **44**(4): p. 832-839.

21. van Jaarsveld, J.G.S. and J.S.J. van Deventer, *Effect of the alkali metal activator on the properties of fly ash-based geopolymers.* Industrial & Engineering Chemistry Research, 1999. **38**(10): p. 3932-3941.

22. Rees, C.A., et al., *The mechanism of geopolymer gel formation investigated through seeded nucleation.* Colloids and Surfaces A: Physicochemical and Engineering Aspects, 2008. **318**(1–3): p. 97-105.

23. Westwick, M.R., Miladin, *The Effect of K/Al and Na/Al ratio on the Structure and Properties of Geopolymers*. 2012, National Science Foundation: Research Experience for Undergraduates.

24. Dombrowski, K., A. Buchwald, and M. Weil, *The influence of calcium content on the structure and thermal performance of fly ash based geopolymers.* Journal of Materials Science, 2007. **42**(9): p. 3033-3043.

25. Xu, H. and J.S.J. van Deventer, *The effect of alkali metals on the formation of geopolymeric gels from alkali-feldspars.* Colloids and Surfaces a-Physicochemical and Engineering Aspects, 2003. **216**(1-3): p. 27-44.

26. Xu, H. and J.S.J. Van Deventer, *Geopolymerisation of multiple minerals.* Minerals Engineering, 2002. **15**(12): p. 1131-1139.

27. van Jaarsveld, J.G.S., J.S.J. van Deventer, and G.C. Lukey, *A comparative study of kaolinite versus metakaolinite in fly ash based geopolymers containing immobilized metals.* Chemical Engineering Communications, 2004. **191**(4): p. 531-549.

28. Perera, D.S., et al., *Influence of curing schedule on the integrity of geopolymers.* Journal of Materials Science, 2007. **42**(9): p. 3099-3106.

29. Duxson, P., et al., *Si-29 NMR study of structural ordering in aluminosilicate geopolymer gels.* Langmuir, 2005. **21**(7): p. 3028-3036.

30. Palomo, A., A. Fernandez-Jimenez, and M. Criado, *"Geopolymers": same basic chemistry, different microstructures.* Materiales De Construccion, 2004. **54**(275): p. 77-91.

31. Zhang, Z., et al., *Geopolymer foam concrete: An emerging material for sustainable construction.* Construction and Building Materials, 2014. **56**: p. 113-127.

32. Duxson, P., G.C. Lukey, and J.S.J. van Deventer, *Thermal conductivity of metakaolin geopolymers used as a first approximation for determining gel interconnectivity.* Industrial & Engineering Chemistry Research, 2006. **45**(23): p. 7781-7788.

33. Kim, K.-H., et al., *An experimental study on thermal conductivity of concrete.* Cement and Concrete Research, 2003. **33**(3): p. 363-371.

34. Bernal, S.A., et al., *Performance of refractory aluminosilicate particle/fiber-reinforced geopolymer composites.* Composites Part B: Engineering, 2012. **43**(4): p. 1919-1928.

35. Temuujin, J., et al., *Preparation and thermal properties of fire resistant metakaolin-based geopolymer-type coatings.* Journal of Non-Crystalline Solids, 2011. **357**(5): p. 1399-1404.

36. Temuujin, J., et al., *Fly ash based geopolymer thin coatings on metal substrates and its thermal evaluation.* Journal of Hazardous Materials, 2010. **180**(1–3): p. 748-752.

37. Bakharev, T., *Thermal behaviour of geopolymers prepared using class F fly ash and elevated temperature curing.* Cement and Concrete Research, 2006. **36**(6): p. 1134-1147.

38. Ali, F.A., D. O'Connor, and A. Abu-Tair, *Explosive spalling of high-strength concrete columns in fire.* Magazine of Concrete Research, 2001. **53**(3): p. 197-204.

39. Davidovits, J., et al. *Geopolymeric cement based on low cost geologic materials. Results from the european research project geocistem*. in *Proceedings of the 2nd International Conference on Geopolymer*. 1999.

40. Skvara, F., *Alkali activated materials or geopolymers?* Ceramics-Silikaty, 2007. **51**(3): p. 173-177.

41. Rostami, H. and W. Brendley, *Alkali ash material: a novel fly ash-based cement.* Environmental science & technology, 2003. **37**(15): p. 3454-3457.

42. Phair, J.W. and J.S.J. Van Deventer, *Effect of silicate activator pH on the leaching and material characteristics of waste-based inorganic polymers.* Minerals Engineering, 2001. **14**(3): p. 289-304.

43. Schwartz, M.M., *Brazing, 2nd Edition*. 2003: ASM International.

44. Permatex. *Technical Data Sheet: Permatex Clear RTV Silicone Adhesive Sealant*. 2003 [cited 2016; Available from: http://www.devcon.com/prodfiles/pdfs/fam_tds_398.pdf.

45. Henkel. *Technical Data Sheet: Loctite Epoxy Weld Bonding Compound*. 2014 [cited 2016; Available from: http://www.loctiteproducts.com/tds/EPXY_WELD_T_tds.pdf.

46. Henkel. *Technical Data Sheet: Loctite Epoxy 1 Minute Instant Mix*. 2014 [cited 2016; Available from: http://www.loctiteproducts.com/tds/EPXY_1MIN_tds.pdf.

47. Armeco. *Technical Data Sheet: High Temperature Ceramic and Graphite Adhesives*. 2015 [cited 2016; Available from: http://www.aremco.com/wp-content/uploads/2015/04/A02_15.pdf.

48. MasterBond, *Technical Data Sheet MASTER BOND MB SERIES CYANOACRYLATES* 2016, Master Bond Inc.: Hackensack, NJ. p. 4.

49. Uehara, K. and M. Sakurai, *Bonding strength of adhesives and surface roughness of joined parts.* Journal of Materials Processing Technology, 2002. **127**(2): p. 178-181.

50. Duxson, P., et al., *The effect of alkali and Si/Al ratio on the development of mechanical properties of metakaolin-based geopolymers.* Colloids and Surfaces a-Physicochemical and Engineering Aspects, 2007. **292**(1): p. 8-20.

51. Steveson, M. and K. Sagoe-Crentsil, *Relationships between composition, structure and strength of inorganic polymers - Part I - Metakaolin-derived inorganic polymers.* Journal of Materials Science, 2005. **40**(8): p. 2023-2036.

52. Steveson, M. and K. Sagoe-Crentsil, *Relationships between composition, structure and strength of inorganic polymers - Part 2 - Flyash-derived inorganic polymers.* Journal of Materials Science, 2005. **40**(16): p. 4247-4259.

53. Temuujin, J., et al., *Preparation of metakaolin based geopolymer coatings on metal substrates as thermal barriers.* Applied Clay Science, 2009. **46**(3): p. 265-270.

54. Latella, B.A., et al., *Adhesion of glass to steel using a geopolymer.* Journal of Materials Science, 2006. **41**(4): p. 1261-1264.

55. Ueng, T.-H., et al., *Adhesion at interface of geopolymer and cement mortar under compression: An experimental study.* Construction and Building Materials, 2012. **35**: p. 204-210.

56. De Barros, S., et al., *Adhesion of Geopolymer Bonded Joints Considering Surface Treatments.* The Journal of Adhesion, 2012. **88**(4-6): p. 364-375.

57. Adachi, M., et al., *Oxide adherence and porcelain bonding to titanium and Ti-6Al-4V alloy.* Journal of dental research, 1990. **69**(6): p. 1230-1235.

58. Özcan, I. and H. Uysal, *Effects of silicon coating on bond strength of two different titanium ceramic to titanium.* Dental Materials, 2005. **21**(8): p. 773-779.

59. Wang, R.R., G.E. Welsch, and O. Monteiro, *Silicon nitride coating on titanium to enable titanium–ceramic bonding.* Journal of Biomedical Materials Research, 1999. **46**(2): p. 262-270.

60. Barbosa, V.F.F. and K.J.D. MacKenzie, *Thermal behaviour of inorganic geopolymers and composites derived from sodium polysialate.* Materials Research Bulletin, 2003. **38**(2): p. 319-331.

61. Butz, R., G.W. Rubloff, and P.S. Ho, *Chemical bonding and reactions at Ti/Si and Ti/oxygen/Si interfaces.* Journal of Vacuum Science & Technology A, 1983. **1**(2): p. 771-775.

62. Ingo, G.M., S. Dirè, and F. Babonneau, *XPS studies of SiO2-TiO2 powders prepared by sol-gel process.* Applied Surface Science, 1993. **70**: p. 230-234.

63. Sergiu Amarie, P.Z., Yusuke Kajihara, Erika Griesshaber, Wolfgang W. Schmahl, Fritz Keilmann1, *Nano-FTIR chemical mapping of minerals in biological materials.* Beilstein J. Nanotechnol., 2012. **2012**(3): p. 312–323.

64. Ren, J., et al., *Silica–Titania mixed Oxides: Si–O–Ti Connectivity, Coordination of Titanium, and Surface Acidic Properties.* Catalysis Letters, 2008. **124**(3): p. 185-194.

65. Swanepoel, J.C. and C.A. Strydom, *Utilisation of fly ash in a geopolymeric material.* Applied Geochemistry, 2002. **17**(8): p. 1143-1148.